UNIVERSITY OF CALIFORNIA
RIVERSIDE

From Ideal to Real: Understanding the Role of Pathogens in the Environment

A Dissertation submitted in partial satisfaction
of the requirements for the degree of

Doctor of Philosophy

in

Chemical and Environmental Engineering

by

Ian Matthew Marcus

March 2013

Dissertation Committee:
Dr. Sharon L. Walker, Chairperson
Dr. Mark R. Matsumoto
Dr. Marylyn V. Yates

The Dissertation of Ian Matthew Marcus is approved:

Committee Chairperson

University of California, Riverside

Acknowledgements

I would first like to thank my committee members: Professor Mark R. Matsumoto (Chemical and Environmental Engineering, UCR) and Professor Marylynn V. Yates (Environmental Science, UCR). When I first came to UCR, I was not well versed in environmental issues, Dr. Matsumoto was very helpful in helping me understand and analyze water quality. When I once said I would like to create different water environments, Dr. Matsumoto said, "Water is water, to simulate different environments just change the solution chemistry", this simple piece of advice saved me a lot of time. Dr. Yates forced me, in the nicest possible way, to narrow my research, so as not be a 10 year Ph.D. Student, as well as provided me invaluable advice with regard to the research to which I am extremely grateful.

My sincere appreciation goes to other researchers who helped along the way, specifically Dr. Mark Ibekwe, for his bacteria help, and giving us strains to play with. Dr. David Crowley for his with understanding genomics, Dr. Morris Maduro for his help with nematodes, and Dr. Abram Aertsen for giving us a plasmid he made. Dr. Moshe Herzberg was a wonderful mentor while in Israel and his consistent bouts of brilliance and his ability to be productive while balancing a huge lab is an inspiration to all aspiring scientists. Dr. Viatchaslav Freger was extremely helpful with understanding certain mathematical models that greatly helped in the production of a manuscript.

I am also grateful to numerous former and current members from Dr. Walker lab group, particularly Dr. Berat Haznedaroglu for bringing me up to speed on working in the

lab and being meticulous with research, Dr. Indranil Chowdhury for being a great roommate, and showing me what good work ethic is all about. Olgun Zorlu for his infectious laugh and consistently great attitude that would always bring my spirit up. Jacob Lanphere and Jessamine Quijano for both helping me before ever joining the lab as graduate students and being wonderful as labmates. Jenia Gutman and Wang Ying for their help in getting acclimated to Israel during my five month stay. Ryan Honda, Sidy Ba, and Troy Ezeh for always remembering life outside of lab when speaking about professional basketball. Dr. Garrett and Dr. Christy Milliron for being the best friends anyone could ask for, always welcoming me into their home and making me feel like I was part of the family. Alicia Taylor for her wonderful smile, always being there when I needed her, and being a truly special friend. Special thanks to the undergraduate researchers worked with me including Brian Perez, Stephen Opot, Alex Duchon, Shanin Quazi, Jose Valle, and irreplaceable always brilliant continuously wonderful Hailey Wilder, whos brilliance never ceased to amaze me. I would like to extend my thanks to the professors in the CEE Department and staff members for their excellent support while GSA president. I am also grateful to Dr. Caroline Li and the late Robert Klevecz of the City of Hope for their excellent mentoring.

I would like to thank my parents for their continuous love and support throughout my life. No matter what profession I was thinking about going into next they would question my motives, and always support every decision.

Finally, I would like to thank my PhD adviser, Dr. Sharon Walker. It would be easy for me to state that how wonderful of adviser and mentor Dr. Walker has been in a

few words, but they would not do justice to what she has meant to me as a person. Whenever meeting with Dr. Walker, no matter how poor of a mood I was in, would always immediately bighten my day, and give me a sense of accomplishment. When I was considering leaving she brought me back with her enthusiasm for my ideas. When things were not looking good abroad in Israel, she motivated me enough to get some interesting results and still have a great time. When I had an opportunity to defend earlier than expected she did not hesitate in her support. That consistent support and enthusiasm is what truly makes Dr. Walker extraordinary and I am extremely grateful to have had the opportunity to work with her.

The research was primarily supported by the USDA, BARD and the UCR Dissertation Year Program fellowship.

Dedication

This dissertation is dedicated to my parents for their consistent love, support, and encouragment through of all of my crazy endeavors.

ABSTRACT OF THE DISSERTATION

From Ideal to Real: Understanding the Role of Pathogens in the Environment

by

Ian Matthew Marcus

Doctor of Philosophy, Graduate Program in Chemical and Environmental Engineering
University of California, Riverside, March 2013
Dr. Sharon L. Walker, Chairperson

The overall goal of this investigation was to elucidate the effects the environment had on pathogenic bacteria in natural and engineered systems. Pathogens are generally studied by growing a single strain in nutrient rich media (ideal conditions), which do not accurately simulate the environments in which these bacteria are found. Thus, this project was developed to show the variations in bacterial phenotype based upon growth phase, to compare the fate and transport of 11 *Escherichia coli* isolates in an idealized media versus a more environmentally representative bovine manure extract, and to move away from the ideal to the real, by simulating representative environments in which pathogen proliferation can occur.

This dissertation work has allowed for the following critical observations to be made. The conditions in which bacteria are grown in the laboratory can significantly alter the cells' physical-chemical and transport properties. Specifically, the growth phase of *Pseudomonas aeruginosa* (PAO1) was the main influence on the relative cell surface hydrophobicity. This in turn changed the mechanism by which the cells adhered to a

quart crystal microbalance with dissipation (QCM-D) sensor surface. Additionally, experiments investigating 11 *E. coli* isolates showed that the solution in which the cells are grown (ideal media vs. real manure extract) has a significant influence on their physical-chemical and transport properties of the bacteria. This work demonstrated the need to study pathogens in conditions that better approximate the complexity of natural systems. Thus, three *in vitro* systems were built to model environments (human colon, septic tank, and groundwater) in which pathogens may be found. A human fecal microbial community was inoculated in the model colon and subsequently into the septic tank and groundwater systems, which led to a change in the microbial community's structure and function. A model pathogen, *E. coli* O157:H7, was added to the systems and was found to significantly impact the microbes present and their resulting fate and transport. This collection of studies confirms the need to study pathogens in simulated systems that more closely represent the real environments in which the cells may proliferate.

Table of Contents

List of Figures

List of Tables

Chapter 1

Introduction

1.1 Motivation and Background

Pathogenic bacteria are a major public health concern in the U.S. and around the world. Pathways in which pathogens infect people include meat consumption by unsanitary slaughter techniques (1,2), fruits and vegetables irrigated with contaminated water (3), and as a result of drinking (4) or swimming in contaminated water (5). The pathogenic strain of *E. coli*, O157:H7, causes dysentery to 73,000 people in the US each year (6). Waterborne diseases from bacterial infections are responsible for 4% of deaths worldwide (7). Though it is much less common to contract waterborne diseases in the developed world, there have been cases of outbreaks in recent years (8-10). Hence, the understanding of the fate and transport of pathogens in the environment is essential to protect drinking, recreational, and agricultural water sources.

One pathway in which pathogens may contaminate water supplies is through decentralized wastewater treatment. About 20% of American households (26 million) and a quarter of planned developments use septic tanks to dispose of their wastewater (11). The US Environmental Protection Agency (EPA) reports that 15% of Americans get their drinking water from onsite groundwater, which is not subject to EPA standards (http://water.epa.gov/type/groundwater/). Decentralized wastewater treatment and using groundwater from personal property are generally self-regulated. This may be problematic since studies have shown that half of U.S. drinking water wells have fecal pollution that causes 750,000-6 million illnesses per year (12). To address this problem, the fate of pathogens in septic systems and groundwater needs to be further investigated.

The common paradigm when studying pathogenic bacteria in the lab has been to grow the cells as a single strain in rich nutrient media and then to harvest and evaluate the organisms' phenotypic and/or genotypic characteristics (13). While this technique has led to a great understanding of the genetics (14) and in showing how the pathogen can infect people (15), this method exposes cells to conditions that the bacteria would not experience in a host organism or aquatic environment. Upon release from the host, the microbial community's dynamics change to adapt to new environmental conditions (16-18). It is a combination of exposure and cellular response that controls the characteristics of the cell when it moves in the environment – both aquatic and terrestrial. It is therefore imperative to study the pathogen as a part of a biological system and to establish the effect the diverse environments and microbial communities have on the pathogen.

This Ph.D. investigation aimed to transform the way in which the contribution of environmental factors on pathogens is considered, specifically in the types of factors that influence the fate and transport of pathogenic bacteria in water. Factors contributing to bacterial transport in the environment include hydrophobic interactions (19-21), surface charge characteristics (21,22), surface macromolecules (23-25), solution chemistry (26-28), cell type (29-31), and growth phase (32-34). These factors were all considered and studied within the framework of this PhD thesis. The first varied condition studied was the growth phase of the bacteria, which lead to a change in hydrophobicity and subsequently an alteration in how cells adhere to surfaces. The second varied condition was the solution in which the bacteria are grown. In this case the growth medium had a major effect on the cell surface characteristics of 11 different isolates. The final stage of

this work – and most novel element of this investigation – included the creation of a model colon, septic tank, and groundwater system together to simulate a potential pathway in which a pathogenic bacterium could potentially infect people by the mechanisms described above (i.e. use of well water for irrigation or drinking). This investigation provides greater insight into how environmental conditions influence the fate and transport of pathogens, which must be taken into consideration when managing water and wastewater treatment options.

1.2 Aim and Scope

The overall objective of this research was to elucidate the impact that environmental parameters have on the phenotype of pathogens. Specifically, this study aims to investigate the fate and transport of pathogens by characterizing bacteria under a spectrum of growth conditions from ideal to real growth conditions. This dissertation addresses this in the three core chapters: investigating the various effects of growth phase (Chapter 2), solution chemistry (Chapter 3), and environmental systems (human colon, septic tank, and groundwater) (Chapter 4) on bacteria phenotype. The aims of this investigation were developed based upon the hypotheses and objectives presented in the subsequent section.

1.3 Hypotheses and Specific Objectives

To achieve the overall goal of this doctoral research, the following hypotheses and specific objectives were developed and are presented below (note that each specific objective has been addressed in a chapter of this dissertation):

Hypothesis 1: The attachment of bacteria onto surfaces will be dependent on cell and surface hydrophobicity.

To test this hypothesis, *P. aeruginosa,* a bacterium often used to model biofilm formation, was grown to mid-exponential and stationary growth phase. The bacteria varied significantly in their degree of hydrophobicity with growth times, while the electrokinetic properties were relatively constant. The bacterial suspension was then injected into a quartz crystal microbalance with dissipation (QCM-D) measurement cell in which the fluid flowed over the sensor. Two sensors with different coatings were used, one hydrophilic and the other hydrophobic. The adherence of the bacteria was monitored using a fluorescent microscope and by the measured shifts in frequency and dissipation. This technique was utilized to determine the role cell and surface hydrophobicity plays in the initial stages of biofilm formation (Chapter 2).

Hypothesis 2: Varying the growth solution from nutrient rich to poor will change the cell surface and transport properties of environmental E. coli isolates.

To test this hypothesis, 11 *E. coli* isolates obtained from a range of agriculturally-relevant environments were grown in LB media (an idealized laboratory growth media)

and bovine manure extract. The properties tested included surface charge density, cell size, hydrophobicity, zeta potential, quantification of extracellular polymeric substances (sugars and proteins), and attachment efficiency of the bacteria. The purpose of this study was to investigate how nutrient conditions influence the fate and transport of microorganisms in the environment (Chapter 3).

Hypothesis 3: The fate (as evaluated by the physical-chemical properties of the pathogen and the microbial community) and transport of pathogenic bacteria will be altered under different environmental conditions.

The overall goal of this investigation is to ascertain the influence that the host microbial community has on pathogens in the environment through commonly encountered systems relevant to water quality. This was done by building *in vitro* lab scale models of a colon, septic tank, and groundwater system. A series of experiments are used to (1) determine the microorganisms present in the three environmentally relevant systems, (2) perform extensive physical-chemical analyses on the community of microorganisms and pathogen (i.e. electrophoretic mobility, cell size, surface charge density, hydrophobicity and extracellular polymeric substances), and (3) test the transport properties of the microbial community in a macroscopic, packed-bed column system. The purpose of this study was to give greater insight into the understanding of the way in which environmental factors influence the fate and transport of pathogenic microorganisms in the environment.

1.4 Experimental Approach

This dissertation is composed of five chapters including the Introduction (Chapter 1) and Conclusion (Chapter 5). Following the Introduction, Chapter 2 describes the impact that cell and surface hydrophobicity have on the attachment of bacteria onto a QCM-D sensor. Specifically, the attachment of *P. aeruginosa* grown to mid-exponential and stationary phase attaching onto bare silica and polyvinylidene fluoride (PVDF) QCM-D sensors were investigated. The investigation presented in this chapter revealed that the cell and surface hydrophobicity had a significant effect on the attachment of the bacteria on the sensor surface, and the resulting viscoelastic properties of the deposited cells. This study is thoroughly described in Chapter 2 entitled, "*Pseudomonas aeruginosa* Attachment on QCM-D Sensors: The Role of Cell and Surface Hydrophobicities".

Chapter 3, entitled "Impact of growth conditions on transport behavior of *E. coli*," investigates the role of growth solution in the fate and transport of 11 environmental *E. coli* isolates. The physical-chemical properties including hydrophobicity, zeta potential, surface charge density, size, and the quantification of extracellular polymeric substances (sugar and protein) were measured for each of the 11 isolates. The results of the extensive phenotypic characterization were then compared to the transport of the cells through packed-bed columns to find possible correlations between the cell characteristics and their transport properties. The growth solutions showed a significant influence on the bacteria cell surfaces and on their transport through packed-bed columns. This study showed the need to consider nutrient conditions when studying bacteria to better mimic

the environmental stresses that bacteria undergo in the natural environment (i.e. in a manure waste).

Chapter 4, entitled "Linking microbial community structure to function in representative simulated systems" describes a novel approach to study pathogenic microorganisms. In this study, a colon, septic tank, and groundwater system were constructed in the laboratory to gain a better understanding of the fate and transport of microbial communities in simulated, relevant environments. A fecal microbial community was inoculated in an *in vitro* colon, the effluent was then allowed to flow into a model septic tank, and the effluent from the septic tank was exposed to artificial groundwater. The microbial community from each of these artificial systems was sampled to test the community composition and phenotypic characteristics (electrophoretic mobility, hydrophobicity, size, extracellular polymeric substances, and attachment efficiency). These characterizations were first done with an unaltered microbial community and then in the presence of a model pathogen, *E. coli* O157:H7, to determine pathogen's effect within the model environments. This study was an initial step in understanding how microbial communities behave in the environment and how resilient the structure and function of the microorganisms are to the presence of a pathogen.

Chapter 5, entitled "Summary and Conclusions" summarizes the findings from this PhD research. The three chapters of this dissertation have been published and are listed below.

1.5 Manuscripts resulted from research

1. Marcus, I.M., Herzberg, M., Walker, S.L., Freger, V. (2012) *Pseudomonas aeruginosa* Attachment on QCM-D Sensors: The Role of Cell and Surface Hydrophobicities, *Langmuir*, **28**, 6396–6402
2. Marcus, I. M., Bolster, C. H., Cook, K. L., Opot, S. R. and Walker, S. L. (2012) Impact of growth conditions on transport behavior of *E. coli*. *Journal of Environmental Monitoring*, **14**, 984-991
3. Marcus, I.M., Wilder, H.A., Quazi, S.J., Walker, S. L., Linking Microbial Community Structure to Function in Representative Simulated Systems. *Applied and Environmental Microbiology.* Accepted for publication 2/1/2013.

1.6 References

1. Wachtel M.R., Whitehand L.C., and Mandrell R.E. (2002) *Journal of Food Protection* **65**, 18-25
2. Weightman, N. C., and Kirby, P. J. G. (2000) *Journal of Hospital Infection* **44**, 107-111
3. Wendel, Arthur M., Hoang Johnson, D., Sharapov, U., Grant, J., Archer, John R., Monson, T., Koschmann, C., and Davis, Jeffrey P. (2009) *Clinical Infectious Diseases* **48**, 1079-1086
4. Akashi, S., Joh, K., Mori, T., Tsuji, A., Ito, H., Hoshi, H., Hayakawa, T., Ihara, J., Abe, T., Hatori, M., Nakamura, T., and Akashi, S. (1994) *European Journal of Pediatrics* **153**, 650-655
5. Keene, W. E., McAnulty, J. M., Hoesly, F. C., Williams, L. P., Hedberg, K., Oxman, G. L., Barrett, T. J., Pfaller, M. A., and Fleming, D. W. (1994) *New England Journal of Medicine* **331**, 579-584
6. Rangel, J. M., Sparling, P. H., Crowe, C., Griffin, P. M., and Swerdlow, D. L. (2005) Epidemiology of Escherichia coli O157:H7 Outbreaks, United States, 1982–2002. DigitalCommons@University of Nebraska - Lincoln
7. Prüss, A., Kay, D., Fewtrell, L., and Bartram, J. (2002) *Environ Health Perspect* **110**

8. Clark, C. G., Price, L., Ahmed, R., Woodward, D.L., Melito, P. L., Rodgers, F.G., Jamieson, F., Ciebin, B., Li, A., Ellis, A. (2003) *Emerg Infect Dis* **9**, 1232-1241

9. Jones IG, R. M. (1996) *Public Health* **110**, 277–282

10. Bopp DJ, S. B., Waring AL, Ackelsberg J, Dumas N, Braun-Howland E, et al. (2003) *J Clin Microbiol* **41**, 174–180

11. EPA, U. S. (2011) Decentralized Wastewater Treatment Systems: Memorandum of Understanding. (Management, O. o. W. ed., 3 Ed.

12. Macler, B. A., and Merkle, J. C. (2000) *Hydrogeology Journal* **8**, 29-40

13. Madigan, M. T., Martinko, J.M. (2006) *Biology of Microorganisms*, 11th ed., Pearson Prentice Hall, Upper Saddle River, N.J.

14. Perna, N. T., Plunkett, G., Burland, V., Mau, B., Glasner, J. D., Rose, D. J., Mayhew, G. F., Evans, P. S., Gregor, J., Kirkpatrick, H. A., Posfai, G., Hackett, J., Klink, S., Boutin, A., Shao, Y., Miller, L., Grotbeck, E. J., Davis, N. W., Lim, A., Dimalanta, E. T., Potamousis, K. D., Apodaca, J., Anantharaman, T. S., Lin, J., Yen, G., Schwartz, D. C., Welch, R. A., and Blattner, F. R. (2001) *Nature* **409**, 529-533

15. Levine, M., and Vial, P. (1988) *Indian Journal of Pediatrics* **55**, 183-190

16. Cook, K. L., and Bolster, C. H. (2007) *Journal of Applied Microbiology* **103**, 573-583

17. Bolster, C. H., Mills, A. L., Hornberger, G. M., and Herman, J. S. (2001) *Journal of Contaminant Hydrology* **50**, 287-305

18. Bolster, C. H., Walker, S.L., Cook, K.L. (2006) *Journal of Environmental Quality* **35**, 1018-1025

19. van Loosdrecht, M. C. M., Lyklema, J., Norde, W., Schraa, G., and Zehnder, A. J. B. (1987) *Appl. Environ. Microbiol.* **53**, 1893-1897

20. Schafer, A., Harms, H., and Zehnder, A. J. B. (1998) *Environ. Sci. Technol.* **32**, 3704-3712

21. Vanloosdrecht, M. C. M., Lyklema, J., Norde, W., Schraa, G., and Zehnder, A. J. B. (1987) *Appl. Environ. Microbiol.* **53**, 1898-1901

22. Gross, M., Cramton, S. E., Gotz, F., and Peschel, A. (2001) *Infect. Immun.* **69**, 3423-3426

23. Kuznar, Z. A., and Elimelech, M. (2005) *Langmuir* **21**, 710-716

24. Kim, H. N., Hong, Y., Lee, I., Bradford, S. A., and Walker, S. L. (2009) *Biomacromolecules* **10**, 2556-2564

25. Kim, H. N., Walker, S. L., and Bradford, S. A. (2010) *Water Res.* **44**, 1082-1093

26. Li, Q., and Logan, B. E. (1999) *Water Res.* **33**, 1090-1100

27. Kuznar, Z., and Elimelech, M. (2004) *Environ. Sci. Technol.* **in press**

28. Bradford, S. A., Kim, H. N., Haznedaroglu, B. Z., Torkzaban, S., and Walker, S. L. (2009) *Environmental Science & Technology* **43**, 6996-7002

29. Walker, S. L. (2005) *Colloid and Surfaces B: Biointerfaces* **45**, 181-188

30. Bolster, C. H., Haznedaroglu, B. Z., and Walker, S. L. (2009) *Journal of Environmental Quality* **38**, 465-472

31. Haznedaroglu, B. Z., Kim, H. N., Bradford, S. A., and Walker, S. L. (2009) *Environmental Science & Technology* **43**, 1838-1844

32. Walker, S. L., Redman, J. A., and Elimelech, M. (2005) *Environmental Science & Technology* **39**, 6405-6411

33. Walker, S. L., Hill, J. E., Redman, J. A., and Elimelech, M. (2005) *Applied and Environmental Microbiology* **71**, 3093-3099

34. Haznedaroglu, B. Z., Bolster, C. H., and Walker, S. L. (2008) *Water Research* **42**, 1547

Chapter 2

Pseudomonas aeruginosa Attachment on QCM-D Sensors: The Role of Cell and Surface Hydrophobicities

Marcus, I.M.; Herzberg, M.; Walker, S.L.; Freger, V. 2012. Pseudomonas aeruginosa Attachment on QCM-D Sensors: The Role of Cell and Surface Hydrophobicities. *Langmuir*. 28 pp. 6396–6402.

Abstract

While biofilms are ubiquitous in nature, the mechanism by which they form is still poorly understood. This study investigated the process by which bacteria deposit and shortly after, attach irreversibly to surfaces by reorienting to create a stronger interaction, which leads to biofilm formation. A model for attachment of *Pseudomonas aeruginosa* was developed using a quartz crystal microbalance with dissipation monitoring (QCM-D) technology, along with a fluorescent microscope and camera to monitor kinetics of adherence of the cells over time. In this model the interaction differs depending on the force that dominates between the viscous, inertial, and elastic loads. *P. aeruginosa,* grown to the mid-exponential growth phase (hydrophilic) and stationary phase (hydrophobic) and two different surfaces, bare quartz (SiO_2), and polyvinylidene (PVDF), which are hydrophilic and hydrophobic, respectively were used to test the model. The bacteria deposited on both of the sensor surfaces, though on the bare quartz surface the cells reached a steady state where there was no net increase in deposition of bacteria, while the quantity of cells depositing on the PVDF surface continued to increase until the end of the experiments. The change in frequency and dissipation per cell were both positive for each overtone (n), except when the cells and surface are both hydrophilic. In the model three factors, specifically viscous, inertial, and elastic loads, contribute to the change in frequency and dissipation at each overtone when a cell

deposits on a sensor. Based on the model, hydrophobic cells were shown to form an elastic connection to either surface, with an increase of elasticity at higher overtones. At lower overtones, hydrophilic cells depositing on the hydrophobic surface, were shown to also be elastic, but as the overtone increases the connection between the cells and sensor becomes more viscoelastic. In the case of hydrophilic cells interacting with the hydrophilic surface, the connection is viscous at each overtone measured, the connection is rigid once the cell deposits on the surface. It could be inferred that the transformation of the viscoelasticity of the cell-surface connection are due to changes in the orientation of the cells to the surface, which allow the bacteria to attach irreversibly and begin biofilm formation.

2.1 Introduction

Microbial biofilms represent an ancient, protected mode of growth that allows microbial survival in hostile environments as well as the ability to disperse and colonize new niches (1). These sophisticated bacterial life forms are widely found on ship hulls (2), power plant piping (3), water supply pipelines (4), irrigation systems (5), and membranes for water purification (6), within the food industry (7), on human implants (8), and in the lungs of cystic fibrosis patients (9). In the majority of these cases, removal of biofilms is difficult and it implies high energetic input (10, 11), application of hazardous chemicals (11), and shutting down of the impacted system (12). Some of the physiological factors that could induce and affect irreversible attachment of bacteria onto a surface include aquatic chemistry, hydrodynamic effects, surface properties, and the physical–chemical properties of the cells.

Biofilms generally form in nutrient-rich environments and remain in biofilm form until the bacteria become nutrient-deprived, which returns the bacteria to a planktonic state (13). A biofilm could form on a surface in laminar or turbulent flow systems, though the properties of the resulting biofilm may differ in extracellular polymeric substance (EPS) content, shear strength (14, 15), and quantity of biomass (16). Previous work has shown that surface hydrophobicity and charge have an effect on initial deposition and attachment of cells onto the surface (17), as does the surface roughness, where a rough surface will enhance the formation of biofilms (18). Hydrophobicity and surface charge

of the cell also have an effect on biofilm formation (1) . While the previously mentioned cell and surface properties have an effect on how biofilms form, in most cases, there are no strategies that could successfully prevent biofilm formation without negative consequences (19).

Within 1 min of bacterial contact with a surface, the bond between the bacteria and the surface strengthens by a factor of 100–1000 (20). Thus, to prevent biofilm formation it is important to understand the transition from the deposition stage, during which there is potential for removal, to the development of irreversible interactions with the surface. The processes by which the cell approaches, deposits, and attaches to the surface may involve hydrodynamic and physical–chemical interactions (21) in the deposition of cells onto the surface. They involve water removal from the cell–surface interface (22) achieving a maximal gain in free energy through increased strength of adhesion as well as coating the surface with extracellular polymeric substances (EPS) from the cells, which form a strong viscoelastic layer (22-25).

A quartz crystal microbalance with dissipation (QCM-D) allows for real-time monitoring of changes in the frequency and dissipation of an adhering mass onto a piezoelectric quartz sensor to assess cell–surface interactions. Negative frequency shifts have been correlated with the addition of rigid mass onto a surface following the classical Sauerbrey relation (26). Although the classical interpretation of a negative frequency as an added mass applies to a rigid planar layer rather than particles (26, 27), it has been used to model bacterial attachment to the surface (28-31) . However, a few recent reports clearly indicated that in some cases the frequency may also increase with the addition of

adherent bacteria (23, 32, 33). Even though this could be explained by a loss of mass from the surface, e.g., via water removal from the contact area, the most common explanation is based on the coupled oscillator model (23, 32-35). This model indicates that in some cases an elastic springlike connection of bacteria (36) or micrometer-size particles (34) to the sensor surface may counterbalance the added inertia and lead to positive frequency shifts. Thus, frequency shift may be misleading as a sole indicator of the amount of bacteria adhering to the surface. In this respect, QCM-D, monitoring changes in dissipation as well as in resonance frequency, allows an insight into viscoelastic and inertial characteristics of the deposited layers (37, 38). Availability of several overtone frequencies is another advantageous feature of QCM-D, since elastic, inertial, and dissipative viscous contributions to frequency and dissipation shifts depend on frequency in a different manner. Thus QCM-D lends insight into adhesion and mechanical coupling between the surface and depositing bacteria as well as their evolution with time until the bacteria are irreversibly attached (23).

The combination of QCM-D with fluorescent microscopy allows for quantifying and visualizing adhered bacteria concurrently with frequency and dissipation monitoring. This approach is applied in this study in order to delineate a mechanism of cell interaction as they approach and deposit on the surface. Olsson et al. used this methodology to study reversible and irreversible attachment of bacteria (23). In that case, surface appendage lengths were varied for a single strain, and attachment was monitored on one specific surface. The present study examines bacterial attachment from a different angle by varying the sensor surface characteristics and growth conditions of the cells. The

experiments employed *Pseudomonas aeruginosa* cells at two different growth phases with a QCM-D utilizing two different sensors coated either with hydrophilic silica (SiO_2) or hydrophobic polyvinylidene fluoride (PVDF). Application of the QCM-D in an experimental matrix combining cells and substrates with different surface characteristics reveals changes occurring at different bacteria–substratum interfaces. These results shed light on the nature of the mechanical elements introduced in the coupled oscillator theory and help connect these elements to the actual characteristics of the cells and their adhesion to the substrate.

2.2 Materials and Methods

2.2.1 **Preparation of Model Bacterial Strain**

Prior to each attachment experiment, a 16 h culture of green fluorescent protein (GFP) labeled *P. aeruginosa* PAO1 (39) was grown in LB (Luria–Bertani) broth by incubation in a shaker–incubator at 150 rpm at 30 °C (ZHWY-1102C, ZHWY). The cells were diluted in LB broth (1:100) and incubated for 5 or 16 h, to achieve midexponential and stationary growth phases, respectively. The growth curve of this strain is presented in Appendix A. Bacteria were harvested by centrifugation (4K15, Sigma) (4000*g* and 4 °C for 10 min) and the pellet was washed three times using a 100 mM NaCl solution (Sigma Aldrich). After harvesting the bacteria, the optical density (OD_{600}) of the suspension was adjusted to 0.1 for all subsequent QCM-D and cell characterization experiments, which corresponds to $(5 \times 10^8) \pm (5 \times 10^6)$ cells mL^{-1}. All characterization and QCM-D

experiments were conducted using cell suspensions in 100 mM NaCl, and all chemicals were ACS grade.

2.2.2 **Characterization of Bacterial Hydrophobicity**

The MATH (microbial adherence to hydrocarbons) method has been described in detail previously (40-42). Briefly, this method is based on the cell partitioning between an electrolyte phase and a hydrocarbon phase. For each experiment, three replicate suspensions (4 mL) from a single bacterial culture were transferred into test tubes containing 1 mL of the hydrocarbon (*n*-dodecane, Sigma Aldrich). The test tubes were vortexed (Vortex Genie 2, Scientific Industries, Bohemia, NY) for 2 min, followed by a 15 min rest period to allow for phase separation. The optical density of the cells in the aqueous phase was measured at OD_{600} (Lambda EZ 201 model, Perkin-Elmer, Waltham, MA) to determine the extent of bacterial cell partitioning. Hydrophobicity values are reported as the percentages of total cells that partitioned into the hydrocarbon. Each MATH experiment was conducted on different days using fresh cultures to ensure reproducibility of results. The average of the six total assays is reported in the Results and Discussion section.

2.2.3 Investigation of Cell Attachment Using QCM-D

QCM-D (Q-sense AB, Gothenburg, Sweden) provides real-time, label-free measurements of molecular adsorption and/or interactions taking place on various

surfaces. In addition to assessing adsorbed mass (ng/cm^2 sensitivity), measured as changes in oscillating frequency (F) of the quartz crystal, the energy dissipation (D), which is the reduced energy per oscillation cycle, provides novel insights regarding structural properties of adsorbed layers. By employing an ultrasensitive coin-shaped quartz mass sensor housed inside a flow cell with well-defined geometry and hydrodynamic characteristics, QCM-D was used to study the initial stages of bacterial deposition and attachment. For each experiment, solutions were added sequentially for a period of time to the QCM-D system using a peristaltic pump (IsmaTec Peristaltic Pump, IDEX, Glattbrugg, Switzerland) operating at a flow rate of 150 μL/min in the following order: (i) distilled deionized water (DDW) for 20 min to establish a baseline of frequency, (ii) 100 mM NaCl background solution for 40 min, (iii) suspended bacteria in the background electrolyte solution for 60 min, (iv) cell-free background electrolyte for 20 min, and (v) DDW for 20 min. Using the Qsoft 401 software (Q-Sense AB, Gothenberg, Sweden), the variations of frequency (Δf) (Hz) and dissipation factor (ΔD) were measured and recorded for six overtones (n = 3, 5, 7, 9, 11, 13) throughout each experiment. Experiments were conducted with two sensor chemistries, gold-coated crystals coated with a polyvinylidene fluoride (PVDF) layer (catalog number QSX999) and silica coated (SiO_2) (catalog number QSX303) prepared by and purchased from Q-Sense (Gothenberg, Sweden). Each experiment was repeated to ensure the reproducibility of the results.

A QCM-D window module was used to verify and quantify the cells attaching to the sensor. Pictures were taken with a camera (Digital Sign DS-2MBW, Nikon) mounted on the fluorescent microscope (Eclipse LV100, Nikon) every 5 min over the course of a 1 h experiment, and images were subsequently processed in Matlab (Mathworks, Natick, MA) (representative images are presented in the Appendix A).

2.2.4 Quartz Sensor Hydrophobicity

The surface hydrophobicity of the two different quartz crystal sensors (silica or PVDF coated) was measured by adding a sessile droplet of DDW at room temperature to the surface and measuring the contact angle using a goniometer (OCA-2, Dataphysics). These angles are measured by taking a picture of the surface immediately after the drop is placed on the surface. Droplets were added to five different locations on the surface to ensure surface homogeneity. The angles of the two ends for each of the droplets are then determined using image processing software (SCAZO Service). These results were averaged to give the values of the sensor surface hydrophobicity.

2.3 Results and Discussion

2.3.1 Surface Characterization

When *P. aeruginosa* culture is harvested at exponential phase, the bacteria are hydrophilic with 22 ± 3% of cell partitioning in *n*-dodecane. At stationary phase, the

bacteria are hydrophobic with 80 ± 3% of cell partitioning in *n*-dodecane (Table 2.1). These results are in accordance with previous research (43). Since midexponential phase are notably more hydrophilic than stationary cells, the cells are heretofore referred to as hydrophilic and hydrophobic when referencing the midexponential and stationary phase cells, respectively. Similarly, the two sensor surfaces used were representative of hydrophilic and hydrophobic ones. Contact angle measurements indicated the silica coated sensor to be moderately hydrophilic (contact angle of 48° ± 2°), and the PVDF coated sensor was hydrophobic (contact angle of 90° ± 4°) (Table 2.1).

Table 2.1. Hydrophobicity of cells and sensor surfaces.

Cell/Sensor	Hydrophobicity*
P. aeruginosa PAO1 (mid-exponential)	22 ± 3%
P. aeruginosa PAO1 (stationary)	80 ± 3%
Silica (SiO_2)	48 ± 2º
Polyvinylidene Fluoride (PVDF)	90 4º

*Units specific to measurement technique, with, % of cells partitioned in hydrocarbon and contact angle in degrees for sensor surfaces.

Electrokinetic properties of the cells and surface have been found previously to affect attachment (44). The results of the zeta potential of the *P. aeruginosa* cells in this study were measured to be −16.4 and −11.1 mV for midexponential and stationary cells, respectively, and the sensors surfaces have a similarly negative charge (−15.1 and −11.6 mV for PVDF and SiO_2, respectively) (18, 45). Utilizing these literature values and the Derjaguin, Landau, Verwey, and Overbeek (DLVO) theory (46), which account for the

electrostatic and van der Waal forces, all of the cell–surface interactions were identified as attractive with no energy barrier to interaction or secondary minima. (Details of the methods, calculations, and results are presented in the Appendix A).

2.3.2 QCM-D Experiments Combined with Fluorescent Microscopy

A QCM-D with a window module attached to a fluorescent microscope and camera was used to quantify cell attachment in real-time for four experimental conditions, *P. aeruginosa* at two different growth phases with the two sensor surfaces. In all of the experiments cells attached; moreover, the initial cell flux (cells min^{-1} cm^{-2}) was fairly close in all cases; i.e., bacteria were depositing at commensurate rates regardless of the type of bacteria and surface. This may suggest that the initial deposition process was governed by diffusive and convective transport of bacteria toward the surface, which mainly depends on their size and is not expected to significantly differ for all cases (47). However, at longer times two different trends emerged, apparently related to the nature of the sensor surface rather than that of the cells. For the two experiments using the silica-coated sensor, cell attachment, as quantified by the microscope images, increased linearly for 20–30 min and then the number of cells attached to the surface plateaued (Figure 2.1). On the other hand, both types of cells deposited onto the PVDF sensor at a steady rate, thereby their number increased linearly for the entire experiment and did not result in a plateau.

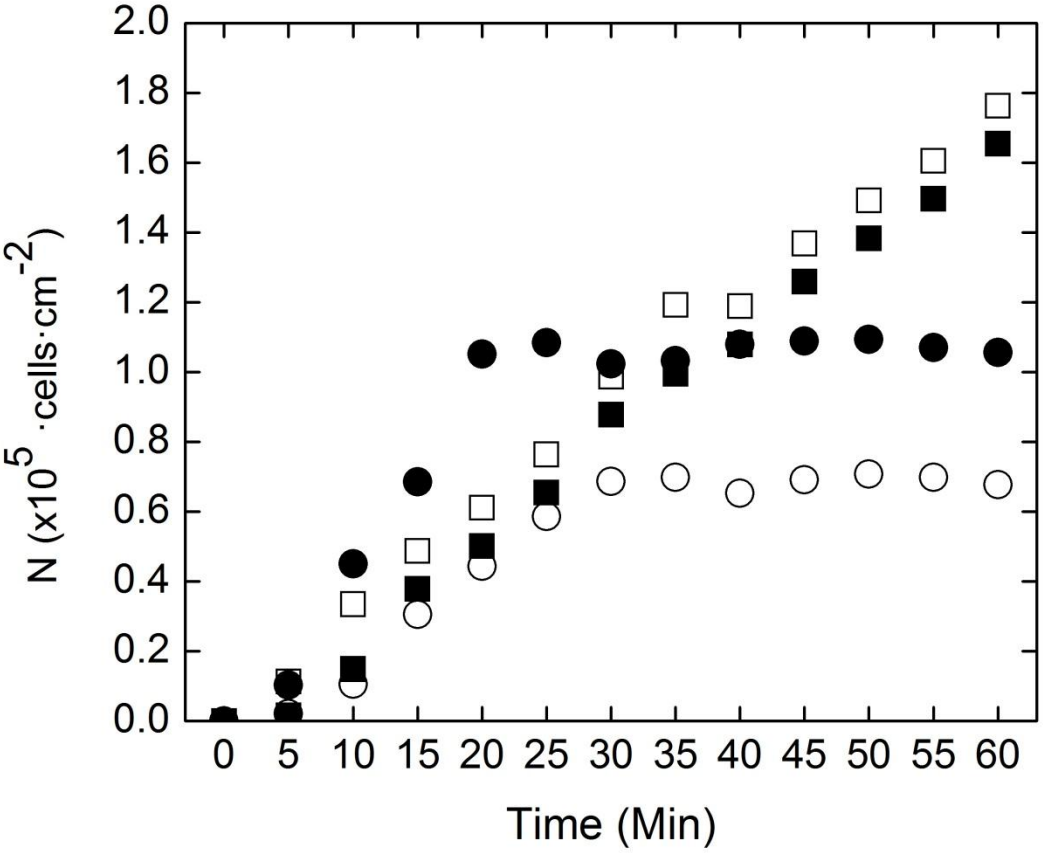

Figure 2.1. Number of cells per cm^2 (N) adhered to the sensor surface over time for hydrophilic (mid-exponential growth phase) cells on a hydrophilic surface (SiO_2) (○), hydrophilic cells on a hydrophobic surface (PVDF) (□), hydrophobic cells (stationary growth phase) on a hydrophilic surface (●), and hydrophobic cells on a hydrophobic surface (■). The reported values are the averages of replicate experiments.

QCM-D data could provide further insight into the mechanism and strength of cell attachment to the two surfaces. Figure 2.2 displays the frequency and dissipation shifts normalized to the number of cells per unit area (cell surface density) at the end of the cell deposition phase as a function of overtone number. In all cases but one, the attachment of bacteria described above resulted in positive frequency shifts at all overtones, as shown

also in previous studies (23, 32, 33). A negative frequency shift expected from the Sauerbrey equation was only observed for the lowest overtones for hydrophilic cells depositing on the hydrophilic SiO_2 surface. Also, the absolute values of the frequency and dissipation shifts were decreasing with overtone number in all cases in a similar manner.

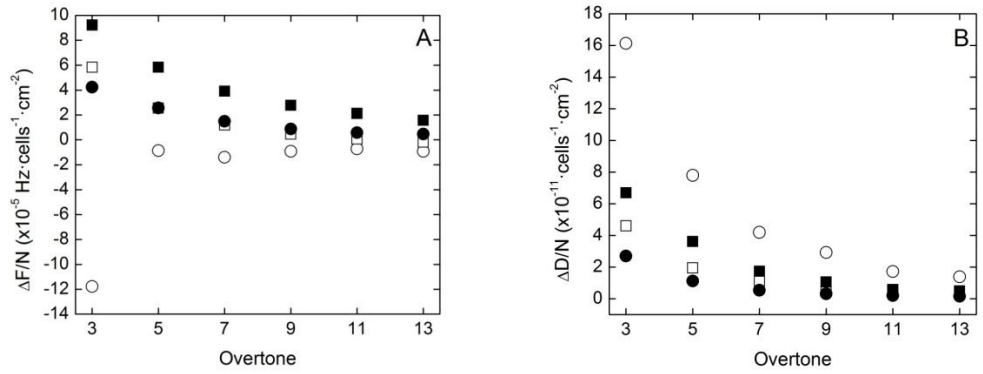

Figure 2.2. Frequency and dissipation shifts normalized to cell surface density versus overtone number (A) Normalized frequency for each surface-cell combination. (B) Normalized dissipation shift for each cell-surface combination. The cell-surface combinations are symbolized as hydrophilic (mid-exponential growth phase) cells on a hydrophilic surface (SiO_2) (○), hydrophilic cells on a hydrophobic surface (PVDF) (□), hydrophobic cells (stationary growth phase) on a hydrophilic surface (●), and hydrophobic cells on a hydrophobic surface (■) for both A and B. The reported values are the averages of replicate experiments.

The QCM-D response is conveniently interpreted using the following relations connecting the shifts in the resonance frequency ΔF and dissipation ΔD with the change of, respectively, the imaginary and real parts of complex load impedance Z_L sensed by QCM. When, as a result of cell adhesion, the load impedance changes by ΔZ_L, the change

in the frequency $F = nf_0$ of the nth overtone and the associated dissipation are given by the following relations (48)

$$\Delta F = -\frac{f_0}{\pi Z_q}\mathrm{Im}(\Delta Z_L) \quad \textbf{(1a)} \qquad \Delta D = \frac{2}{\pi n Z_q}\mathrm{Re}(\Delta Z_L) \quad \textbf{(1b)}$$

where f_0 = 5 MHz is the fundamental frequency of the crystal, Z_q the load impedance of the free crystal equal to 8.8×10^6 kg m^{-2} s^{-1} for AT-cut quartz crystal, n the overtone number, and $\mathrm{Re}(\Delta Z_L)$ and $\mathrm{Im}(\Delta Z_L)$ designate the real and imaginary parts of ΔZ_L, respectively. The change ΔZ_Lshould be proportional to the number of deposited cells and the difference in Z_L per unit area associated with a deposited cell, which may be expressed as follows

$$\Delta Z_L = NA(Z_C - Z_F) \quad \textbf{(2)}$$

where N is the surface density of deposited cells, A is the sensor area associated with an individual deposited cell (thus NA is the sensor area associated with *all* deposited cells), and Z_C and Z_F are the load impedances per unit area associated, respectively, with an individual deposited cell and with the cell-free sensor in the fluid (water) relative to free unloaded crystal in vacuum.

Since the density of the deposited cells N was different in all cases, it is more appropriate to compare normalized shifts $\Delta F/N$ and $\Delta D/N$, representative of the average interaction between an individual cell and the surface, rather than absolute values ΔF and ΔD. However, even the normalized shifts $\Delta F/N$ and $\Delta D/N$ might not be straightforward

to use, if one has to address the variation of the shifts with the overtone, since overtone dependence might be affected by the nonuniformity of the oscillation amplitude. In particular, due to stronger energy trapping at larger overtones (49), cells could contribute unequally across the sensor and the degree of nonuniformity would vary for each overtone. Thus, it may be beneficial to look at the ratio $\Delta F/\Delta D$, in which both N and nonuniformity are canceled out, thereby it becomes a truly inherent characteristics of the specific individual cell deposited on the particular surface. The ratio $\Delta F/\Delta D$ or its reciprocal are often used to measure the relative rigidity of deposit material on the sensor in a simpler case of planar deposit layers (50, 51).

The normalized shifts $\Delta F/N$ and $\Delta D/N$ as well as the ratio $\Delta F/\Delta D$ as function of the overtone number are presented in Figures 2.2 and 2.3. The interpretation is facilitated by noting the following:

(1) For a free crystal in liquid, both imaginary and real parts of Z_F are equal, positive, and inversely proportional to the fluid penetration depth δ that is in turn inversely proportional to $F^{-1/2}$ and hence also $n^{-1/2}$. This means $\mathrm{Im}(Z_F) = \mathrm{Re}(Z_F) \sim n^{1/2}$; therefore $\Delta F/N \sim -n^{1/2}$, $\Delta D/N \sim n^{-1/2}$, and $\Delta F/\Delta D \sim -n$ (see eqs 1a and 1b). As noted before, the dependence of $\Delta F/N$ and $\Delta D/N$ on n may be distorted by nonuniform oscillation, but that of $\Delta F/\Delta D$ should not.

(2) Since the cell diameter is about 1 μm, it is much larger than $\delta \sim 100$ nm, and then $\mathrm{Re}(Z_C) > \mathrm{Re}(Z_F)$; i.e., the dissipation by the cell, which may be assumed

to be similar to that of an oscillating sphere (52), should be larger than that of bare crystal but still related to δ and n in a similar manner. $\Delta D/N$ should then be always positive upon cell deposition and decrease with overtone in about the same manner ($\Delta D/N \sim n^{-1/2}$) for all cells and surfaces.

(3) According to the coupled-oscillator model (34, 36), $\mathrm{Im}(Z_C)$ and ΔF are determined by two counteracting contributions, inertia of the cell and spring elasticity of the connection between the surface and cell; this connection may be assumed to behave as an elastic spring. The intertia increases $\mathrm{Im}(Z_C)$ and leads to a negative ΔF, while the springlike elastic connection produces an opposite effect. The absolute values of inertial and elastic loads have a different dependence on the overtone number. Namely, for inertia $\Delta F \sim -n$ and $\Delta F/\Delta D \sim -n^{3/2}$, i.e., negative with absolute value *increasing* with n, and for elastic load $\Delta F \sim +n^{-1}$ and $\Delta F/\Delta D \sim +n^{-1/2}$, i.e., positive with absolute value *decreasing* with n.

(4) The overall ΔF is determined by the way the dissipative, inertial, and elastic loads are connected within Z_C and their values relative to Z_F (see Figure 2.4 and eq 2). Since the elastic connection is the one that transmits the force from the sensor to the cell, the suggested mechanical circuit for Z_C is shown in Figure 2.5, which also compares it with the circuit of clean crystal (Z_F). In Figure 2.4, for elements connected in-series, the displacement is the

same and forces are added up (i.e., complex impedances are added up), while for elements connected in parallel, the force is the same and displacements are added up. Thus, one should add up reciprocal impedances to obtain total reciprocal impedance.

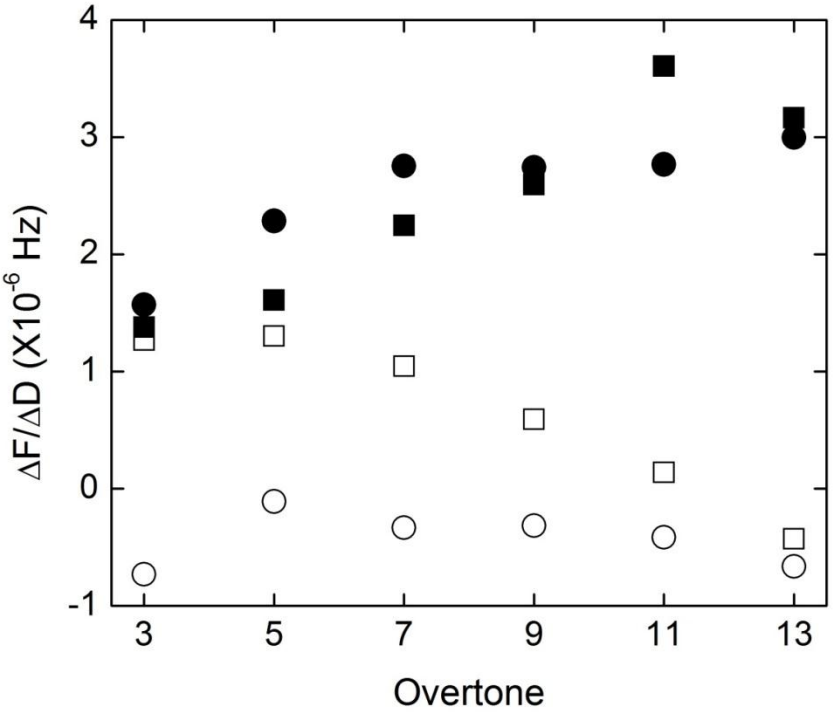

Figure 2.3. Slopes of frequency divided by dissipation at the point in the experiments where there is no increase in cell deposition on the surface. Slopes are presented for each surface-cell combination versus overtone number as follows, hydrophilic (mid-exponential growth phase) cells on a hydrophilic surface (SiO_2) (○), hydrophilic cells on a hydrophobic surface (PVDF) (□), hydrophobic cells (stationary growth phase) on a hydrophilic surface (●), and hydrophobic cells on a hydrophobic surface (■) for both A and B. The reported values are the averages of replicate experiments.

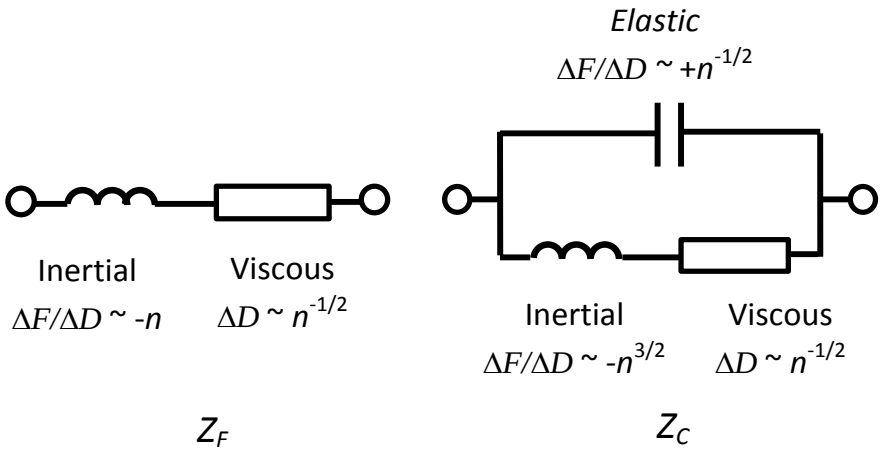

Figure 2.4. The equivalent circuits for the mechanical load impedances of clean crystal Z_F (left) and of the crystal area associated with a single deposited cell Z_C (right) showing connection and overtone-dependence of viscous, inertial and elastic loads.

2.3.3 Hydrophobic Cells Firmly Attach and Induce Elastic Load on the Sensor

For the hydrophobic cells, the behavior is similar, regardless of the sensor's surface, $\Delta F/\Delta D$ being positive and moderately increases with n. The positive $\Delta F/N$ and $\Delta F/\Delta D$ for hydrophobic cells clearly point to the dominance of the elastic load. Apparently, the parameter $\Delta F/\Delta D$moderately increases with n, which may be explained by eq 2 and the equivalent circuit in Figure 2.4. Indeed, the overall response is determined by the difference between Z_C and Z_F. If $Z_C$is mainly elastic, the overall $\Delta F/\Delta D$ should approximately behave as $C_1 n^{-1/2} + C_2 n$, where prefactors C_1 and C_2 are both positive and may vary in each case depending on dissipation, strength of elastic

connection, cell rigidity, fluid viscosity, etc. The faster changing second term, C_2n, could be responsible for the elevated $\Delta F/\Delta D$ with n for hydrophobic cells.

The relatively high magnitude of $\Delta F/\Delta D$ in the case of hydrophobic cells compared to hydrophilic cells (Figure 2.3) implies that a firm elastic connection is formed. Water release from the cell–surface interface was suggested previously to take part in increasing the strength of cell contact with the surface (22), which is likely to play a role in this case. Note that in the case of hydrophobic cell attachment, surface hydrophobicity had no effect on this interaction, with a relatively similar $\Delta F/\Delta D$. Apparently, once a firm contact is established, the elastic contribution is determined only by rigidity of the cell.

2.3.4 Hydrophilic Cells May Not Firmly Attach to the Surface

Interestingly, hydrophilic cells depositing on PVDF showed a trend opposite to hydrophobic cells depositing on either surface; $\Delta F/\Delta D$ was lower and also moderately decreased with n. Apparently, elastic loading dominates also in the case of hydrophilic cells deposition on hydrophobic surface. In this case, the equivalent circuit in Figure 2.4 cannot explain the decrease in $\Delta F/\Delta D$ with n. It seems that in this case, Z_C crosses over from elastic ($+n^{-1/2}$) behavior to more rapidly increasing inertial load ($-n^{3/2}$) as n increases; however, since inertia and elasticity are parallel, the *smaller* one, i.e., elasticity, should actually dominate according to Figure 2.4, but that is not observed. The proposed explanation is that a *firm connection*between the sensor and hydrophilic cell could not be fully established, i.e., the connection was*viscoelastic*,

through a finite liquid gap separating the cell and surface, rather than elastic and becomes predominantly viscous as n increases. As a result, the elastic branch could be deactivated with increasing n and inertia took over as the dominant term contributing to ΔF, as indeed observed.

The same argument may be extended to the case when both surface and cells were hydrophilic. In this case, it may be assumed that the connection was even weaker, i.e., negligibly elastic and was mainly through viscous shear forces; thus, the elastic branch in the circuit in Figure 2.4 was largely deactivated. As expected and seen in Figure 2.3, for hydrophilic cells depositing on the SiO_2 surface, across all overtones, the $\Delta F/\Delta D$ is the lowest among all combinations. The absence of a strong elastic connection is consistent with the lowest slope under these conditions and rapid saturation of N versus time in Figure 2.1. Since penetration depth, δ, decays with n, the viscous connection was most efficient for the lowest, third overtone, where moderate negative shifts in $\Delta F/N$ and $\Delta F/\Delta D$ were observed. The negative shift is consistent with the negligible elastic contribution. For larger overtones ($n > 3$), $\Delta F/N$ was close to zero; however, $\Delta D/N$ was larger compared to other surface-cell combinations. Presumably, without an elastic bond to the sensor, the cells were nearly motionless; thus, compared to other cases, the viscous shear and dissipation increased due to viscous friction of a liquid gap between the motionless cell and moving surface. It should be noted that in the case of attachment of hydrophilic cell, higher slopes of $\Delta F/\Delta D$ were observed for PVDF compared to SiO_2. This difference can be explained by a faster release of water from the cell–surface interface and formation a more elastic and rigid bacteria–PVDF surface connection.

2.4 Conclusions

In general, a positive frequency shift was shown to occur for interactions involving hydrophobic surfaces, i.e., when either cells or sensor surface or both were hydrophobic. Under these conditions, a relatively firm elastic cell–surface connection is suggested to govern, and intuitively, it could be presumed that higher hydrophobic interaction may induce more water molecules to leave the surface, being replaced with the attached cell wall components. Interestingly, the highest dissipation shifts per cell surface density were observed for the combination of hydrophilic cells and hydrophilic surface. It may be deduced that the cells under these conditions were nearly motionless; thus, the viscous shear and dissipation increased due to a thin liquid gap remaining between the cell and sensor surface.

The highest contribution of attached cells to the increase in the sensor frequency is shown for the combination of hydrophobic cells and the hydrophobic PVDF, where it was shown that elastic load dominates. Lower and similar contribution to the increase in the sensor frequency is shown for the combinations of hydrophobic surface and hydrophilic cells as well as hydrophilic surface and hydrophobic cells. For the case of hydrophobic cells on hydrophilic surface, the study shows that still elastic load dominates, as observed by the elevation of ratio $\Delta F/\Delta D$ as a function of n. In contrast, for the case of hydrophilic cells on hydrophobic surface, the connection between the sensor and the cells becomes more viscous as n increases. Finally, for the combination of

hydrophilic cells and hydrophilic SiO_2, $\Delta F/\Delta D$ is the lowest and the viscous connection dominates.

This investigation has led to the understanding of bacterial attachment and the role of cell and surface hydrophobicity in the type of cell–surface connection. It could be hypothesized that further transient changes in the viscoelastic characteristics of the cell–surface connection can be attributed to reorientation and molecular rearrangements (including removal of interfacial water) after cell deposition. This speculated reorientation of bacteria after deposition can ensure the ability of the cells to firmly attach to the surface and form a biofilm.

In order to reduce microbial attachment and control biofilm growth, extensive efforts have been devoted to the development of antifouling surfaces during the past decade. Better understanding of the viscoelastic properties of the contact between microorganisms and such novel surfaces will probably enable us to predict the mechanical strength of this contact and, therefore, to improve biofilm control strategies.

2.5 References

1. O'Toole, G., Kaplan, H. B., and Kolter, R. (2000) *Annual Review of Microbiology* **54**, 49-79
2. Tribou, M., and Swain, G. (2009) *Biofouling* **26**, 47-56
3. Sriyutha Murthy, P., Venkatesan, R., Nair, K. V. K., and Ravindran, M. (2004) *International Biodeterioration & Biodegradation* **53**, 133-140
4. Lazarova, V., and Manem, J. (1995) *Water Research* **29**, 2227-2245
5. Huang, T. Y., Gulabivala, K., and Ng, Y. L. (2008) *International Endodontic Journal* **41**, 60-71
6. Pang, C. M., Hong, P., Guo, H., and Liu, W.-T. (2005) *Environmental Science & Technology* **39**, 7541-7550
7. Chmielewski, R. A. N., and Frank, J. F. (2003) *Comprehensive Reviews in Food Science and Food Safety* **2**, 22-32
8. Donlan, R. M. (2001) *Clinical Infectious Diseases* **33**, 1387-1392
9. Costerton, J. W. (2001) *Trends in Microbiology* **9**, 50-52
10. Gibson, H., Taylor, J. H., Hall, K. E., and Holah, J. T. (1999) *Journal of Applied Microbiology* **87**, 41-48
11. Simões, M., Pereira, M. O., and Vieira, M. J. (2005) *Water Research* **39**, 5142-5152
12. Lund, V., and Ormerod, K. (1995) *Water Research* **29**, 1013-1021

13. Costerton, J. W., Lewandowski, Z., Caldwell, D. E., Korber, D. R., and Lappin-Scott, H. M. (1995) *Microbial biofilms*, Annual Reviews

14. Vrouwenvelder, J. S., van Loosdrecht, M. C. M., and Kriuthof, J. C. (2011) *Water Research* **45**, 2880-3898

15. Vrouwenvelder, J. S., Buiter, J., Riviere, M., van der Meer, W. G. J., van Loosdrecht, M. C. M., and Kruithof, J. C. (2010) *Water Research* **44**, 689-702

16. Simoes, M., Pereira, M. O., Sillankorva, S., Azeredo, J., and Vieira, M. J. (2007) *Biofouling* **23**, 249-258

17. Boks, N. P., Kaper, H. J., Norde, W., van der Mei, H. C., and Busscher, H. J. (2009) *Journal of Colloid and Interface Science* **331**, 60-64

18. Pasmore, M., Todd, P., Smith, S., Baker, D., Silverstein, J., Coons, D., and Bowman, C. N. (2001) *Journal of Membrane Science* **194**, 15-32

19. Simões, M., Simões, L. C., and Vieira, M. J. (2010) *LWT - Food Science and Technology* **43**, 573-583

20. Vadillo-Rodríguez, V., Busscher, H. J., Norde, W., de Vries, J., and van der Mei, H. C. (2004) *Journal of Colloid and Interface Science* **278**, 251-254

21. Torkzaban, S., Bradford, S. A., and Walker, S. L. (2007) *Langmuir* **23**, 9652-9660

22. Busscher, H. J., and Weerkamp, A. H. (1987) *FEMS Microbiology Letters* **46**, 165-173

23. Olsson, A. L. J., van der Mei, H. C., Busscher, H. J., and Sharma, P. K. (2010) *Langmuir* **26**, 11113-11117

24. Dalton, H. M., Goodman, A. E., and Marshall, K. C. (1996) *Journal of Industrial Microbiology & Biotechnology* **17**, 228-234

25. Fletcher, M. (1996) *Bacterial adhesion: molecular and ecological diversity*, Wiley-IEEE

26. Sauerbrey, G. (1959) *Zeitschrift für Physik A Hadrons and Nuclei* **155**, 206-222

27. Höök, F., Rodahl, M., Brzezinski, P., and Kasemo, B. (1998) *Langmuir* **14**, 729-734

28. Otto, K., Elwing, H., and Hermansson, M. (1999) *J. Bacteriol.* **181**, 5210-5218

29. Serra, B., Gamella, M., Reviejo, A., and Pingarrón, J. (2008) *Analytical and Bioanalytical Chemistry* **391**, 1853-1860

30. Pavey, K. D., Barnes, L. M., Hanlon, G. W., Olliff, C. J., Ali, Z., and Paul, F. (2001) *Letters in Applied Microbiology* **33**, 344-348

31. Nivens, D. E., Chambers, J. Q., Anderson, T. R., and White, D. C. (1993) *Analytical Chemistry* **65**, 65-69

32. Olofsson, A.-C., Hermansson, M., and Elwing, H. (2005) *Appl. Environ. Microbiol.* **71**, 2705-2712

33. Olsson, A. L. J., van der Mei, H. C., Busscher, H. J., and Sharma, P. K. (2008) *Langmuir* **25**, 1627-1632

34. Pomorska, A., Shchukin, D., Hammond, R., Cooper, M. A., Grundmeier, G., and Johannsmann, D. (2010) *Analytical Chemistry* **82**, 2237-2242

35. Dybwad, G. L. (1985) *Journal of Applied Physics* **58**, 2789-2790

36. Olsson, A. L. J., van der Mei, H. C., Busscher, H. J., and Sharma, P. K. (2011) *Journal of Colloid and Interface Science* **357**, 135-138

37. de Kerchove, A. J., and Elimelech, M. (2006) *Biomacromolecules* **8**, 113-121

38. Ying, W., Yang, F., Bick, A., Oron, G., and Herzberg, M. (2010) *Environmental Science & Technology* **44**, 8636-8643

39. Banin, E., Lozinski, A., Brady, K. M., Berenshtein, E., Butterfield, P. W., Moshe, M., Chevion, M., Greenberg, E. P., and Banin, E. (2008) *Proceedings of the National Academy of Sciences* **105**, 16761-16766

40. Bolster, C. H., Cook, K. L., Marcus, I. M., Haznedaroglu, B. Z., and Walker, S. L. (2010) *Environmental Science & Technology* **44**, 5008-5014

41. Pembrey, R. S., Marshall, K. C., and Schneider, R. P. (1999) *Appl. Environ. Microbiol.* **65**, 2877-2894

42. Rosenberg, M., Gutnick, D., and Rosenberg, E. (1980) *FEMS Microbiology Letters* **9**, 29-33

43. Herzberg, M., Rezene, T. Z., Ziemba, C., Gillor, O., and Mathee, K. (2009) *Environmental Science & Technology* **43**, 7376-7383

44. Walker, S. L., Hill, J. E., Redman, J. A., and Elimelech, M. (2005) *Appl. Environ. Microbiol.* **71**, 3093-3099

45. Redman, J. A., Walker, S. L., and Elimelech, M. (2004) *Environmental Science & Technology* **38**, 1777-1785

46. Hermansson, M. (1999) *Colloids and Surfaces B: Biointerfaces* **14**, 105-119

47. Elimelech, M., Gregory, J., Jia, X., and Williams, R. A. (1995) Particle Deposition and Aggregation: Measurement, Modeling and Simulation. Butterworth-Heinemann. pp 441

48. Johannsmann, D. (2008) *Physical Chemistry Chemical Physics* **10**, 4516-4534

49. Reviakine, I., Morozov, A. N., and Rossetti, F. F. (2004) *Journal of Applied Physics* **95**, 7712-7716

50. Notley, S. M., Eriksson, M., and Wågberg, L. (2005) *Journal of Colloid and Interface Science* **292**, 29-37

51. Schofield, A. L., Rudd, T. R., Martin, D. S., Fernig, D. G., and Edwards, C. (2007) *Biosensors and Bioelectronics* **23**, 407-413

52. Landau, L. D., and Lifshitz, E. M. (1959) *Fluid Mechanics, translated by J. B. Sykes and W. H. Reid*, Pergamon Press, Oxford

Chapter 3

Impact of growth conditions on transport behavior of *E. coli*

Marcus, I. M.; Bolster, C. H.; Cook, K. L.; Opot, S. R.; Walker, S. L. 2012. Impact of growth conditions on transport behavior of E. coli. *Journal of Environmental Monitoring*. **14:**984-991.

Abstract

The aim of this investigation is to determine the effect that growth solution has on the cell surface properties and transport behavior of eleven *Escherichia coli* isolates through saturated porous media. The two growth solutions used were a standard laboratory growth medium (LB) and a dairy manure extract solution. In general, cells grown in manure extract were more hydrophobic, had a more negative zeta potential, had lower amounts of surface macromolecules, and had lower attachment efficiencies than isolates grown in LB. An inverse relationship between the natural log of zeta potential and the attachment efficiency of the isolates for the cells grown in LB media was the only statistically significant correlation observed between transport behavior and cell characteristics of the isolates. This study shows the need to consider growth conditions when studying bacteria to better mimic the environmental stresses that bacteria undergo in the natural environment. This approach could lead to a better understanding of the behavior of manure-derived bacteria in aquatic and terrestrial environments.

3.1 Introduction

Contamination from fecal matter is the leading cause of impairment of potable water sources in the US (1). *Escherichia coli* are the most commonly identified fecal indicator bacteria (FIB) originating from agricultural and urban runoff (2), and are used as an indicator of water quality. While the indicator bacteria can be used to determine whether fecal contamination occurred, the association between *E. coli* and the targeted pathogenic bacteria has been found to be weak (3). These pathogens include *Campylobacter, Salmonella,* and virulent strains of *Escherichia coli* (4, 5). Pathogenic bacteria shed from livestock have the potential to reach potable water sources, including groundwater, from farms via storm runoff or in manure that has been treated for reuse (6)**.** Another route for introduction is manure from farm animals used as a fertilizer for agricultural crops (7), which could contaminate the farm produce with pathogenic bacteria (8). Hence, understanding the fate and transport of various strains of *E. coli* originating from agricultural waste is essential for assessing water quality and protecting drinking, recreational, and agricultural water sources from contamination.

Previous work has utilized highly idealized conditions to investigate microbial fate and transport. For example, when studying *E. coli* in the laboratory, growth media such as LB (lysogeny broth) is often used to provide a consistent nutrient source for the organisms to grow. Such growth media are designed and tested to ensure reproducible and predictable growth conditions (9). This laboratory technique has led to an improved understanding of the genetics of *E. coli* (10), demonstrating how pathogens can infect

people (11), mechanisms of bacterial transport (12), and biofilm formation (13, 14). However, nutrient-rich growth media are not representative of the conditions that the organisms will be exposed to once expunged from the intestines of farm animals. Therefore, to understand the fate and transport of *E. coli* originating from agricultural waste – or any other microorganism of interest – it is essential that the organisms are grown in more representative media.

Previous studies have made an effort to link cell surface properties to the transport of the microorganisms in the environment. Notably cell type (15-19), size (20-22), hydrophobic interactions (15, 18, 21, 23, 24), surface charge (18, 22, 23, 25-28), and surface macromolecular content (29-31) have been measured. However, relatively few studies have investigated the link between cell characteristics and transport behavior of cells grown in manure solutions. Cellular characteristics such as zeta potential and hydrophobicity have been shown to differ for cells grown in either manure or other idealized laboratory environments such as bovine intestinal conditions (32, 33). Yang et al. reported that among the isolates that they tested, four had higher attachment efficiency when grown in manure, while two isolates had lower attachment efficiency (33). These trends show that the fate and transport of bacteria isolates are affected by composition of the growth media.

In addition to the growth conditions of cells, the presence of manure in bacterial transport can have an effect on their adhesion properties. The attachment of the bacteria to soil particles is greatly reduced when the cells are suspended with manure as opposed to cells suspended in an electrolyte suspension (34-36). The attachment of the cells

suspended in manure to negatively charged soil may be hindered 7, since they may tend to attach better to positively charge inorganic particles that may aid their transport (37). These reported trends suggest the presence of manure during bacterial transport may allow pathogenic bacteria to be transported to a greater extent. This suggests studies without manure may be underestimating movement of bacteria in groundwater.

To address this notable gap in the literature, a study was developed to compare and evaluate the differences in the fate and transport of cells that were grown in either a dairy manure extract solution or more traditional laboratory media (LB). Eleven *E. coli* isolates from dairy manure were extensively characterized using physical and chemical techniques. Additionally, transport studies were conducted with the organisms after growth in one of the two test media. Results allow for an assessment of whether the typical laboratory practice of using a standard growth media is adequate for simulating and predicting bacterial fate and transport in manure contaminated aquatic environments.

3.2 Materials and Methods

3.2.1 *E. coli* isolation and isolate selection

Five 1-L samples of dairy manure slurry (i.e., mixture of manure, urine, and straw) were collected from a manure pit located on the farm at Western Kentucky University. The samples were collected at five randomly chosen locations within the pit using 1-L sterilized Nalgene bottles attached to an adjustable sampling pole. The samples

were returned to the laboratory and processed immediately. Ten mL from each 1-L bottle were serially diluted to 10^{-6} in phosphate buffer. One hundred µl from each dilution was plated onto m-Tech plates and incubated at 44.5 ºC for 24 hr. Following incubation, each presumptive *E. coli* colony (i.e. purple colony) was plated on EMB and mFC agar. This yielded a total of 339 presumptive *E. coli* colonies. *E. coli* isolates were fingerprinted by BOX PCR analysis as previously described except the initial denaturation step was extended to 12 min (38). Briefly, Rep-PCR using 0.5 µM of the BOX AIR primer (5'-CTACGGCAAGGCGACGCTGACG-3') (BOX-PCR) was carried out in a 25 µl reaction containing 1X EconoTaq PLUS master mix (Lucigen, Middleton, WI) and 2 µl of diluted cell suspension. The PCR was conducted on a PTC-200 model thermal cycler (MJ Research/BioRad, Hercules, CA) and PCR mixtures (10 µl) were electrophoresed on 1% agarose gel supplemented with 40% synergel (Diversified Biotech, Boston, MA) for 4 hr at 75 V. Ethidium bromide stained gel images were captured in quadrants with a FOTO/Analyst Investigator/Eclipse system (Fotodyne Inc., Hartland, WI). Bands were identified and the data were statistically analyzed using Fingerprinting II Software Version 3.0 (BioRad, Hercules, CA). DNA fingerprints were compared using the Jaccard method for calculating similarity coefficients, cluster analyses of similarity matrices were performed by an unweighted pair group method with arithmetic mean (UPGMA) and isolates were grouped into unique BOX-PCR profiles based on 80% similarity in BOX-PCR fingerprint pattern as previously described (39). Eleven isolates were chosen from the major fingerprint groups to be used in the column studies. Each of the isolates was further confirmed to be *E. coli* by chemical analysis using Enterotube

following the manufacturer's directions and by PCR analysis of the *uidA* gene as previously described (40). All isolates were stored at -80 ºC with 15% glycerol.

3.2.2 Isolate typing and evaluation of fimH and agn43

The eleven isolates were placed into one of four phylogenetic groups (A, B1, B2, or D) using the triplex PCR method of Clermont et al. (41) as modified by Higgins et al. (42). The PCR program was 15 min at 94 ºC, 29 cycles at 94 ºC for 30 s, 55 ºC for 30 s and 72 ºC for 30 s. PCR analyses for the presence of *agn43* and *fimH* were carried out as previously described [43]. The touchdown PCR conditions for the *agn43* reaction consisted of an initial cycle of 95 °C for 15 min; 10 cycles of 94 °C for 30 s, 72 °C to 62 °C for 60 s, and 72 °C for 30 s, and 35 cycles of 94°C for 30 s, 62 °C for 60 s and 72 °C for 30 s. The PCR program for *fimH* was 15 min at 95 ºC, 35 cycles of 94 ºC for 30 s, 60 ºC for 60 s, and 72 ºC for 30 s followed by a final extension at 72 °C for 5 min. All assays were carried out in Qiagen HotStart Taq Master Mix (Qiagen, Valencia, CA) in a total volume of 25 µl with 2 µl of genomic DNA extract and 0.5 µM primer in a PTC-200 model thermal cycler (MJ Research/BioRad, Hercules, CA). PCR mixtures (10 µl) were electrophoresed on 1% agarose gel 1 hr at 75 V. Ethidium bromide stained gel images were captured with a FOTO/Analyst Investigator/Eclipse system (Fotodyne Inc., Hartland, WI). Primer sequences, product size, and targeted genes are shown in Table 3.1.

3.2.3 Manure extract preparation

Manure extract was prepared by mixing 40 g fresh dairy manure with 1 L of synthetic precipitation solution (EPA Method 1312) (44) for one hr using a roller. The resulting slurry was centrifuged at 2900 x g for 20 min. The decanted solution was filtered twice through a 0.45 µm filter and stored at 4 C in the dark. Immediately prior to use, 0.01 % yeast extract was added and the mixture filtered through a 0.45 µm filter.

3.2.4 Cell preparation

The eleven isolates selected were individually streaked on LB-Miller agar plates and grown in a 37 °C incubator overnight. Single colonies were picked from the LB plates and allowed to grow in 5 mL vials at 37 °C for 12 hr to achieve stationary phase. The cells were diluted (1:100 ratio with deionized water (DI)) and 200 µl of the diluted cell culture were placed into a 200 mL flask of either manure extract, with 0.01% weight/volume of yeast extract, or LB media. This subsequent culture was incubated at 37 °C until stationary phase. Next the liquid cell culture was centrifuged to separate the cells from the growth media at 3700 x g for 15 min at 4 °C (Eppendorf 5810R, Germany). The cell pellet was resuspended in 10 mM KCl solution prepared with DI and reagent grade KCl (Fisher Scientific, Pittsburgh, PA) with no pH adjustment (pH 5.6−5.8). This process was repeated twice in order to ensure complete removal of the growth medium prior to further analyses.

3.2.5 Cell surface characterization

The extracellular polymeric substance (EPS) composition, cell size, electrophoretic mobility, hydrophobicity, and surface charge density were measured for each isolate using previously published methods (28). All of the cell surface analyses described below used 10 mM KCl as the background solution, unless stated otherwise.

To quantify the extracellular polymeric substance on the cell surface, the pellet of harvested bacterial cells was suspended in formaldehyde-NaCl solution. After two hr the fixed cells were centrifuged, washed with DI water, and sonicated for three min. The cell pellet was then placed in a -80 ºC freezer followed by freeze drying for six hr before the colorimetric test (45). After diluting the pellet in DI water triplicate assays were made for sugar and protein analysis. The protein and sugar were measured spectroscopically (BioSpec-mini, Shimadzu Corp., Kyoto, Japan) using the Lowry Method (46) at 500 nm and phenol-sulfuric acid method (47) at 480 nm, respectively.

Cell size was measured from images taken using a phase contrast microscope (Micromaster; Fisher Scientific, Pittsburgh, PA) and camera. Images containing significant number of cells (each with >50) were processed by image processing software (Matlab, The MathWorks, Inc., Natick, MA) and individual cell lengths and widths were determined.

A zeta potential analyzer (Brookhaven Instruments Corporation, Holtsville, NY) was used to determine the electrophoretic mobility of the cell isolates. After suspending the cells in 10 mM KCl, as described above, the bacterial solution was diluted to an

optical density of ~0.2 at a wavelength of 546 nm. The measurements were repeated five times for three assays taken from the diluted bacterial stock solution and the average was reported. Electrophoretic mobility values that were measured were converted to zeta potential values using the Smoluchowski equation (48).

Hydrophobicity analysis of the bacteria was done by using the microbial adhesion to hydrocarbon (MATH) test (49). The bacteria were first diluted to an optical density of ~0.2 at a wavelength of 546 nm. One mL of a hydrocarbon, n-dodecane (Fisher Scientific) was added to three assays of 4 mL of the diluted bacteria suspension and each of the assays were vortexed for 2 min. The partitioning of cells between n-dodecane, and the electrolyte solution (10 mM KCl) was then determined spectroscopically at 546 nm after 15 min. The relative hydrophobicity was calculated as the percent of total cells partitioned into the hydrocarbon phase.

The surface charge density and relative acidity of the bacterial surfaces were determined by conducting potentiometric titration with the isolates. Bacterial suspensions with concentrations of 10^8-10^9 cells/mL in 10 mM KCl were titrated by concentrated NaOH (0.1 N) from pH 4-10 using an auto-titrator (798 MPT Titrino, Metrohm, Switzerland). Surface charge density and acidity were calculated by knowing the amount of base consumed to change the pH of the solution from 4 to 10 (50).

3.2.6 Transport experiments

Transport experiments were conducted using water-saturated columns packed with clean quartz sand (Unimin^{TM}, New Caanan, CT) that passed through a 850 µm sieve

and was collected on a 710 µm sieve (U.S.A. Standard Testing Sieves, ATM Corp., New Berlin, WI). The sand was boiled in a 2-L flask containing 1 M hydrochloric acid (Fisher Scientific) for 2 hr and then rinsed with DI water until the rinse water pH was ~5.6. The sand was then dried in an oven overnight at 105 °C, re-rinsed in DI water the following day, and dried again overnight at 105 °C. Finally, the sand was sterilized by autoclaving at 121 °C and 15 psi for 20 min. Columns were wet packed by slowly pouring the clean, autoclaved sand into 2.5-cm diameter Chromaflex™ Chromatography Columns (Kontes Glass Co., Vineland, NJ) while vibrating the columns. Columns ranged in length from 9.9 to 10.1 cm. After packing was completed, a 10 mM electrolyte solution was pumped through the columns in an upward direction using syringe pumps (Model 200 syringe pump, KD Scientific Inc., New Hope, PA), and approximately 10 pore volumes (PV) of the electrolyte solution were passed through each column to equilibrate the sand pack. Columns were operated at a flow rate of 0.67 mL min^{-1} for a Darcian velocity of ~ 0.36 cm min^{-1}.

Following equilibration, a 38 min pulse (~ 1.2 PV) of an *E. coli* bacterial solution was passed through each column followed by 75 min of a bacteria free electrolyte solution. Concentrations of *E. coli* in the influent and effluent were determined by plating the appropriate dilutions on mFC Agar plates (Difco Laboratories Inc., Detroit MI) and incubating overnight at 37 ^{o}C. The *E. coli* concentration in the influent was ~ 2 (±1) x 10^{6} colony forming units (CFUs) per mL. Three bulk effluent samples were collected from each column to determine the total number of cells which passed through the 10 cm columns. The three samples were collected after ~ 0.8, 2.2, and 3.2 PV. The fractional

recovery of each *E. coli* isolate was calculated from the total number of cells collected in the second sample and the total number of cells introduced into the column. The dimensionless bacterial deposition rate, κ, was then calculated from the relative recovery by (51):

$$\kappa = \left[-\ln(fr) + \left(\frac{\ln(fr)^2}{Pe} \right) \right] \qquad \textbf{[1]}$$

where *fr* is the fractional recovery defined as the number of bacteria recovered in the column effluent normalized by the total number of bacteria introduced into the system and *Pe* is the hydrodynamic Peclet number of the fluid (dimensionless). The Peclet number in our columns is estimated to be 110 based on bromide tracer tests conducted in an earlier study using similarly packed columns[28]. The bacterial attachment efficiency was calculated from the deposition rate using the hemispheres-in-cell model derived by Ma et al. (52):

$$\alpha = \frac{2d_c}{3(1-\varepsilon)} \frac{\kappa}{L} \frac{1}{\eta} \left[\frac{3-\varepsilon}{3-3\varepsilon} - \frac{2(3-\varepsilon)}{\pi(3-3\varepsilon)} \cos^{-1}\left(\frac{3-3\varepsilon}{3-\varepsilon} \right)^{1/2} + \frac{2}{\pi} \sqrt{2\left(\frac{3-\varepsilon}{3-3\varepsilon} \right)^{-1/2} - 1} \right]^{-1} \quad [2]$$

where α is the bacterial attachment efficiency, d_c is the sand grain diameter (cm), ε is porosity, L is column length (cm), and η is the single-collector efficiency calculated using the correlation equation of Ma et al. (52) assuming a bacterial density of 1055 kg m^{-3} and a Hamaker constant of 6.5 x 10^{-21} J (53). Every transport experiment was repeated on a separate day using a different culture to ensure true replication.

3.2.7 Statistical analysis

Differences in cell surface properties, fractional recoveries, and sticking efficiencies between LB- and manure-grown cells were statistically analyzed using Fisher's LSD method with no adjustment for multiple comparisons. All statistical analyses were performed using JPM ver 7.0 (SAS Institute, 2007) and differences were considered significant at $p < 0.05$.

3.3 Results and Discussion

3.3.1 Isolate selection and genetic characterization

Selective plating and BOX PCR analysis of DNA extracts were conducted on the *E. coli* obtained from dairy pit slurry. Using a threshold of 80 % similarity in BOX fingerprint patterns, 11 unique profiles were differentiated from the 339 *E. coli* isolates. Eleven isolates, representing 94 % of the diversity of diary *E. coli* isolates were selected for transport studies and cell surface characterization. The genotyping triplex assay of Clermont et al. (41) was used to place the 11 *E. coli* isolates into one of the four main phylogenetic groups (A, B1, B2 and D). Based on this analysis, five of the dairy isolates grouped with the B1 genotype, four grouped with the D genotype and two with group A (Table 3.1). All of the isolates were positive for the *fimH* and all except two (DP2D08, DP4B09) were positive for *agn43*; two well-known adhesion factors (21, 32). These results are consistent with a previous study of 1,346 *E. coli* isolates from livestock manures and agriculturally impacted waters (39). In that study, *fimH* (present in 80% to

95% of isolates) and *agn43* (present in 40% to 100% of isolates) were the most commonly detected genes of eleven targets associated with adhesion, transport and virulence.

Table 3.1. Type distribution and genetic characterization of E. coli isolates. The genotypes as well as the presence and absence of a few key adhesion factors are listed for each isolate. +/- denotes presence and absence of gene, respectively.

	DP1 A04	**DP1 F07**	**DP1 H11**	**DP2 D08**	**DP2 G06**	**DP3 B05**	**DP3 D01**	**DP3 F07**	**DP4 B04**	**DP4 B09**	**DP4 F12**
Triplex Geno-type	**D**	**D**	**B1**	**B1**	**B1**	**B1**	**B1**	**A**	**D**	**D**	**A**
uidA	+	+	+	+	+	+	+	+	+	+	+
fimH	+	+	+	+	+	+	+	+	+	+	+
agn43	+	+	+	-	+	+	+	+	+	-	+

3.3.2 Cell surface properties of the bacterial isolates

An extensive list of measured cell properties of isolates grown in LB or manure are displayed in Table 3.2 and 3.3. For eight of the eleven isolates, hydrophobicity was greater for the manure extract grown cells compared with the LB grown cells (eight of these were significant at $P < 0.05$). The range of hydrophobicity values for the cells grown under the two different conditions were similar, 25-85% and 24-84% for isolates grown in the dairy manure extract and LB, respectively. This trend is similar to previous work with *E. coli* grown in manure versus a more nutrient rich environment (32), when the strains were more hydrophobic when grown in manure, or did not change at all.

All of the isolates had a negative zeta potential, ranging between -5 to -32 mV, and -6 to -46 mV for the cells grown in LB and manure, respectively. The zeta potentials for six isolates were significantly more negative ($P < 0.05$) when grown in manure as compared with cells grown in LB. This greater magnitude of charge renders these cells more stable in suspension and potentially capable of greater transport when conditions are unfavorable for bacterial attachment to surfaces (54). Only one isolate, DP4F12, was significantly less negative ($P < 0.05$) when grown in manure. Four of the isolates showed no significant difference in zeta potential between the two growth solutions. These organisms had zeta potential values less negative than -10mV, except for DP2G06, which had values of -28 and -27 mV for cells grown in LB and manure, respectively. The range of zeta potential values of these isolates is similar to previously published research irrespective of growth conditions **(**21, 22, 28, 32)**.**

Table 3.2 displays the calculated values of surface charge density. This is a measure of the distribution of polar functional groups exposed on the cell surface as determined from the experimentally determined acidity level and subsequently calculated charge density (50). While there was no noticeable trend in surface charge density values between the two growth conditions, the range in values between isolates was greater for the cells grown in the manure extract than in LB (80-977 $\mu C/cm^2$ versus 123-533 $\mu C/cm^2$, respectively). These ranges in values are typical of *E. coli* isolates **(**22, 28).

Table 3.2. Comparison of the cell surface properties of E. coli isolates obtained from dairy cattle manure grown in the lab using LB media and manure extract. The values displayed include the average value of the experiments and the standard deviations are in parentheses.

	Hydrophobicity (%)		**Zeta Potential (mV)**		**Surface Charge Density ($\mu C/cm^2$)**	
Isolate	LB	Manure	LB	Manure	LB	Manure
DP1A04	46 (9.8)	75* (2.7)	-7.2 (0.3)	-30* (2.2)	244	179
DP1F07	38 (11)	76* (7.7)	-8.6 (0.1)	-25* (0.4)	192	166
DP1H11	34 (3.0)	74* (20)	-33 (0.7)	-46* (5.2)	224	80
DP2D08	24 (8.6)	80* (1.8)	-12 (0.1)	-21* (1.6)	127	292
DP2G06	67 (8.2)	75 (4.1)	-28 (1.1)	-27 (1.7)	123	104
DP3B05	84 (2.5)	60* (3.5)	-5.8 (0.9)	-31* (3.8)	212	82
DP3D01	34 (6.9)	50* (5.3)	-5.4 (2.5)	-20* (4.7)	396	116
DP3F07	77 (6.7)	75 (1.3)	-9.6 (2.1)	-9.1 (0.1)	160	276
DP4B04	31 (3.3)	25* (0.8)	-6.1 (1.1)	-8.5 (0.8)	127	646
DP4B09	25 (11)	63* (5.0)	-7.1 (2.3)	-6.8 (0.3)	225	977
DP4F12	83 (3.6)	85 (2.9)	-14 (3.6)	-7.9* (0.2)	533	731

*Differences between cells grown in manure extract and LB that exceed Fisher's LSD of 13.8 for hydrophobicity and 4.57 for zeta potential ($P = 0.05$).

For each isolate the extracellular polymeric substances (EPS) content was measured (Table 3.3). Levels of total EPS, as well as sugar and protein, were significantly lower ($P < 0.05$) for cells that were grown in manure as compared to those grown in LB. Notably, bacteria grown in LB media had approximately an order of magnitude higher sugar content than cells grown in the manure extract (0.78-2.55 mg

sugar/10^{10} cells and 0.09-0.30 mg sugar/10^{10}cells, respectively). A similar trend was observed for protein, with cells grown in LB having 26.6-94.7 mg protein/10^{10} cells, and cells grown in manure extract having 0.63-10.47 mg protein/10^{10} cells.

Table 3.3. Comparison of the extracellular polymeric substances on E. coli isolates obtained from dairy cattle manure grown in the lab using LB media and manure extract. The values displayed include the average value of the experiments and the standard deviations are in parentheses.

	Mean Sugar (mg/10^{10} cell)		Mean Protein (mg/ 10^{10} cell)	
Isolate	**LB Media**	**Manure Extract**	**LB Media**	**Manure Extract**
DP1A04	1.34 (0.01)	0.12* (0.003)	43.1 (0.7)	2.33* (0.4)
DP1F07	1.40 (0.05)	0.09* (0.001)	52.2 (1.4)	1.98* (0.3)
DP1H11	0.84 (0.01)	0.15* (0.003)	26.6 (0.1)	1.90* (0.7)
DP2D08	1.05 (0.04)	0.12* (.0006)	39.0 (0.9)	0.65* (0.05)
DP2G06	2.24 (0.2)	0.30* (.0007)	91.4 (0.5)	0.63* (0.3)
DP3B05	2.36 (0.02)	0.16* (0.02)	85.6 (2.2)	2.27* (0.5)
DP3D01	1.33 (0.01)	0.25* (0.005)	39.2 (0.3)	3.57* (0.7)
DP3F07	1.55 (0.04)	0.27* (0.003)	56.1 (2.5)	3.05* (0.5)
DP4B04	0.78 (0.02)	0.28* (0.005)	28.8 (2.5)	10.47* (0.5)
DP4B09	1.13 (0.02)	0.13* (0.005)	40.4 (2.4)	2.86* (0.2)
DP4F12	2.55 (0.06)	0.30* (0.01)	94.7 (5.3)	0.63* (0.06)

*Differences between cells grown in manure extract and LB that exceed Fisher's LSD of 0.312 for sugar concentration and 2.65 for protein concentration (P = 0.05).

These measured cell properties for the 11 *E. coli* dairy isolates confirm that *E. coli* exhibit very different behavior when grown in LB broth as compared to dairy manure extract (Tables 3.2 and 3.3). Four isolates (DP1A04, DP1F07, DP1H11, and DP3D01) showed complementary trends, including a higher absolute zeta potential value, increased hydrophobicity, and decreased surface charge density in manure, compared with cells grown in LB media. The cell properties of DP2D08 were similar to the previously mentioned four isolates except the surface charge density was higher when grown in the

manure extract. DP3F07 and DP4B04 did not vary between the media types with regard to zeta potential and hydrophobicity, but both had higher surface charge density when grown in manure. DP2G06 cell properties did not vary between the media types with regard to zeta potential and hydrophobicity, but had a slightly lower surface charge density when grown in the manure extract. DP3B05 became more hydrophobic and had a higher absolute value of zeta potential, and a lower surface charge density when grown in manure extract. DP4B09 was more hydrophobic, had a similar zeta potential, and had a higher surface charge density when grown in manure extract. DP4F12 had similar hydrophobicity, lower zeta potential, and higher surface charge density when grown in manure extract. Each isolate had much lower level of EPS on a per cell basis, for both sugar and protein content, when grown in manure extract than when they are grown in LB media (Table 3).

3.3.3 Growth media influence on transport

The fractional recovery (*fr*) of the *E. coli* isolates eluted from the 10-cm columns ranged from 0.32 to 0.67 for cells grown in dairy manure extract and 0.36 to 0.65 for cells grown in LB broth (Table 3.4). Calculated bacterial attachment efficiencies (α) ranged from 0.33 to 0.82 for manure extract grown cells and 0.33 to 0.73 for LB grown cells (Table 3.5). Nine of the eleven isolates had lower fractional recoveries (3 to 32 % lower) and higher attachment efficiencies (6 to 86 %) when grown in LB broth compared

with dairy manure extract. Differences between growth conditions exceeded Fisher's LSD ($P < 0.05$) for *fr* for five isolates (Table 3.4) and α for six isolates (Table 3.5).

The range in bacterial attachment efficiencies among the different *E. coli* isolates observed in this study was lower than the range observed for eight isolates obtained from a swine lagoon using similarly packed columns (28). In that study α values varied by over an order of magnitude for stationary phase cells grown in LB broth whereas in this study α values varied by a factor of less than three. One possible explanation for the reduced range in α is that a 10 fold higher ionic strength electrolyte solution was used in the current study. When conditions become more favorable for deposition, as would occur with an increase in ionic strength, the diversity in α among *E. coli* isolates is expected to decrease (28).

Table 3.4. Measured fractional recoveries for E. coli grown in LB broth and dairy manure extract.

Isolate	Manure	LB	Δfr[1]
DP1A04	0.45	0.47	0.019 (4.2)
DP1F07	0.54	0.40	-0.14 (-26)*
DP1H11	0.67	0.64	-0.033 (-5.0)
DP2D08	0.60	0.58	-0.017 (-2.9)
DP2G06	0.59	0.53	-0.052 (-8.9)
DP3B05	0.47	0.38	-0.090 (-19)*
DP3D01	0.46	0.36	-0.10 (-22)*
DP3F07	0.63	0.43	-0.21 (-32)*
DP4B04	0.47	0.41	-0.062 (-13)
DP4B09	0.49	0.41	-0.082 (-17)*
DP4F12	0.32	0.36	0.042 (13)

[1] Differences in fractional recovery (*fr*) between the two growth treatments (Δfr) with percent differences between treatments in parentheses. Significant differences which exceed Fisher's LSD of 0.068 ($P = 0.05$) are denoted with an asterisk.

Table 3.5. Calculated attachment efficiencies for E. coli grown in LB broth and dairy manure extract.

Isolate	Manure	LB	$\Delta\alpha$[1]
DP1A04	0.427	0.423	-0.004 (-0.9)
DP1F07	0.332	0.488	0.156 (46.8)*
DP1H11	0.209	0.237	0.028 (13.2)
DP2D08	0.292	0.307	0.015 (5.1)
DP2G06	0.319	0.320	0.001 (0.3)
DP3B05	0.403	0.494	0.091 (22.5)*
DP3D01	0.448	0.566	0.118 (26.3)*
DP3F07	0.234	0.453	0.219 (93.4)*
DP4B04	0.393	0.454	0.061 (15.4)
DP4B09	0.368	0.477	0.109 (29.6)*
DP4F12	0.583	0.519	-0.064 (-11.0)

[1] Differences in attachment efficiencies (α) between the two growth treatments ($\Delta\alpha$) with percent differences between treatments in parentheses. Significant differences which exceed Fisher's LSD of 0.10 (P = 0.05) are denoted with an asterisk.

In order to explain the differences in transport behavior we observed among the different *E. coli* isolates, the correlation between the attachment efficiency and the different cell surface properties reported above was investigated. The only statistically significant correlation observed was between the zeta potential and attachment efficiency of the cells grown in LB media (Figure 3.1). Interestingly, the best-fit line relating attachment efficiency with the natural log of the zeta potential has a slope (-0.13) very similar to the one reported previously for swine *E. coli* isolates conducted under similar experimental conditions but with a 10-fold lower ionic strength solution (-0.11). This relationship, however, did not hold for cells grown in dairy manure extract. This suggests that cell characteristics controlling the transport of *E. coli* through porous media vary depending on composition of the growth media. Thus, results from experiments

utilizing *E. coli* grown in commercial media may not be directly applicable to *E. coli* movement in the environment.

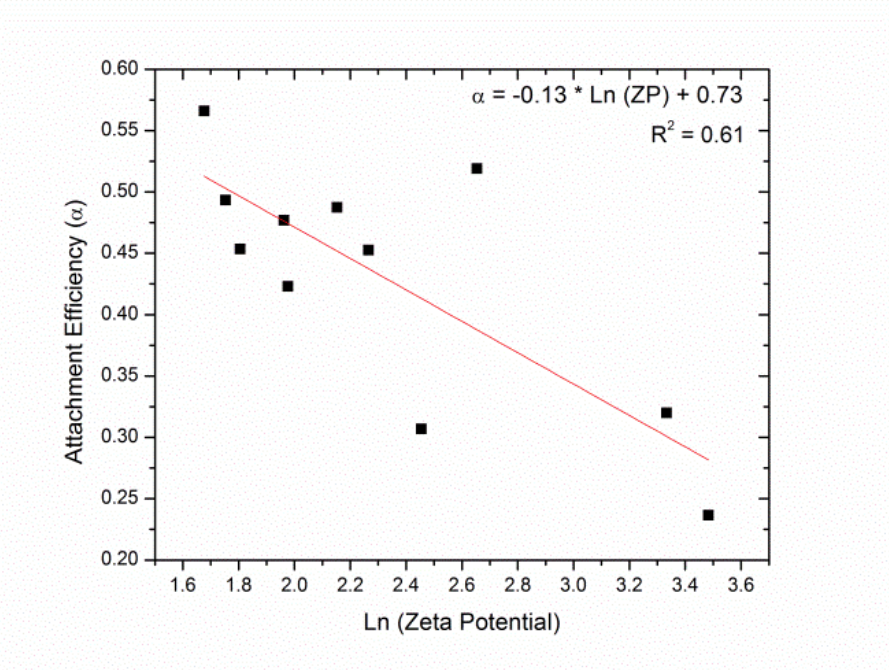

Figure 3.1. Relationship between the natural log of zeta potential and the attachment efficiency for isolates grown in LB media.

3.4 Conclusions

This study has investigated the differences in the cell surface and transport properties of cells that were grown in dairy manure extract and more traditional laboratory media (LB). Notably the cells grown in manure were more hydrophobic, had a more negative zeta potential, less EPS, and had a lower attachment efficiency than the isolates grown in LB. The cell surface properties and attachment efficiencies of the 11 *E. coli* dairy isolates demonstrated the standard laboratory practice of using a single isolate

and standard growth media (LB) is insufficient for simulating transport of *E. coli* from a manure source. Future research is needed to adequately model the fate and transport of bacteria grown in more representative growth solutions. Using isolates from other livestock grown in their respective manure sources should be considered to give a more accurate portrayal of the transport properties of the indicator bacteria used to track the pathogens, to ensure they do not reach ground and surface water.

3.5 References

1. EPA, U. S. (2004) National Water Quality Inventory Report EPA.
2. Macler, B. A., and Merkle, J. C. (2000) *Hydrogeology Journal* **8**, 29-40
3. Meays, C. L., Broersma, K., Nordin, R., and Mazumder, A. (2004) *Journal of Environmental Management* **73**, 71-79
4. Mawdsley, J. L., Bardgett, R. D., Merry, R. J., Pain, B. F., and Theodorou, M. K. (1995) *Applied Soil Ecology* **2**, 1-15
5. Hinton, M., and Bale, M. J. (1991) *Anglais* **70**, 81-90
6. Gerba, C. P., and Smith, J. E. (2005) *Journal of Environmental Quality* **34**, 42-48
7. Pachepsky, Y. A., Sadeghi, A. M., Bradford, S. A., Shelton, D. R., Guber, A. K., and Dao, T. (2006) *Agricultural Water Management* **86**, 81-92
8. Solomon, E. B., Potenski, C. J., and Matthews, K. R. (2002) *Journal of Food Protection* **65**, 673-676
9. Elbing, K., and Brent, R. (2002) *Current Protocols in Molecular Biology*, 3rd ed.,
10. Perna, N. T., Plunkett, G., Burland, V., Mau, B., Glasner, J. D., Rose, D. J., Mayhew, G. F., Evans, P. S., Gregor, J., Kirkpatrick, H. A., Posfai, G., Hackett, J., Klink, S., Boutin, A., Shao, Y., Miller, L., Grotbeck, E. J., Davis, N. W., Lim, A., Dimalanta, E. T., Potamousis, K. D., Apodaca, J., Anantharaman, T. S., Lin, J., Yen, G., Schwartz, D. C., Welch, R. A., and Blattner, F. R. (2001) *Nature* **409**, 529-533
11. Levine, M., and Vial, P. (1988) *Indian Journal of Pediatrics* **55**, 183-190

12. Castro, F. D., and Tufenkji, N. (2008) *Environmental Science & Technology* **42**, 9178-9183

13. Pratt, L. A., and Kolter, R. (1998) *Molecular Microbiology* **30**, 285-293

14. Reisner, A., Haagensen, J. A. J., Schembri, M. A., Zechner, E. L., and Molin, S. (2003) *Molecular Microbiology* **48**, 933-946

15. van Loosdrecht, M. C., Lyklema, J., Norde, W., Schraa, G., and Zehnder, A. J. (1987) *Applied Environmental Microbiology* **53**, 1893-1897

16. Gannon, J. T., Manila, V. B., and Alexander, M. (1991) *Applied Environmental Microbiology* **57**, 190-193

17. Becker, M. W., Metge, D. W., and Collins, S. A. (2003) *Ground Water* **41**, 682-689

18. Walczak, J. J., Bardy, S. L., Feriancikova, L., and Xu, S. (2011) *Water, Air, & Soil Pollution* **222**, 305-314

19. Stumpp, C., Lawrence, J. R., Hendry, M. J., and Maloszewski, P. (2011) *Environmental Science & Technology* **45**, 2116-2123

20. Bradford, S. A., Simunek, J., and Walker, S. L. (2006) *Water Resources Research* **42**, 1-12

21. Lutterodt, G., Basnet, M., Foppen, J. W. A., and Uhlenbrook, S. (2009) *Water Research* **43**, 595-604

22. Bolster, C. H., Haznedaroglu, B. Z., and Walker, S. L. (2009) *Journal of Environmental Quality* **38**, 465-472

23. van Loosdrecht, M. C., Lyklema, J., Norde, W., Schraa, G., and Zehnder, A. J. (1987) *Applied Environmental Microbiology* **53**, 1898-1901

24. Schäfer, A., Ustohalb, P., Harmsa, H., Staufferb, F., T. Dracosb, T., and Zehnder, A. J. B. (1998) *Journal of Contaminant Hydrology* **33**, 149-169

25. Gross, M., Cramton, S. E., Götz, F., and Peschel, A. (2001) *American Society for Microbiology* **69**, 3423-3426

26. Dong, H., Onstotta, T. C., Kob, C., Hollingsworth., A. D., Brown, D. G., and Maillouxa, B. J. (2002) *Colloids and Surfaces B: Biointerfaces* **24**, 229-245

27. Soon, R. L., Nation, R. L., Cockram, S., Moffatt, J. H., Harper, M., Adler, B., Boyce, J. D., Larson, I., and Li, J. (2011) *Journal of Antimicrobial Chemotherapy* **66**, 126-133

28. Bolster, C. H., Cook, K. L., Marcus, I. M., Haznedaroglu, B. Z., and Walker, S. L. (2010) *Environmental Science & Technology* **44**, 5008-5014

29. Jucker, B. A., Zehnder, A. J. B., and Harms, H. (1998) *Environmental Science & Technology* **32**, 2909-2915

30. Burks, G. A., Velegol, S. B., Paramonova, E., Lindenmuth, B. E., Feick, J. D., and Logan, B. E. (2003) *Langmuir* **19**, 2366-2371

31. Kim, H. N., Bradford, S. A., and Walker, S. L. (2009) *Environmental Science & Technology* **43**, 4340-4347

32. Yang, H.-H., Morrow, J. B., Grasso, D., Vinopal, R. T., and Smets, B. F. (2006) *Environmental Science & Technology* **40**, 6976-6982

33. Yang, H.-H., Morrow, J. B., Grasso, D., Vinopal, R. T., Dechesne, A., and Smets, B. F. (2008) **42**, 9310-9316

34. Guber, A. K., Shelton, D. R., and Pachepsky, Y. A. (2005) *Vadose Zone Journal* **4**, 828-837

35. Guber, A. K., Pachepsky, Y. A., Shelton, D. R., and Yu, O. (2007) *Appl. Environ. Microbiol.* **73**, 3363-3370

36. Bradford, S. A., Tadassa, Y. F., and Pachepsky, Y. A. (2006) *Journal of Environmental Monitoring* **35**, 749-757

37. Chowdhury, I., Cwiertny, D. M., and Walker, S. L. (2012) *Environmental Science & Technology* **46**, 6968-6976

38. Dombek, P. E., Johnson, L. K., Zimmerley, S. T., and Sadowsky, M. J. (2000) *Appl. Environ. Microbiol.* **66**, 2572-2577

39. Cook, K. L., Bolster, C. H., Ayers, K. A., and Reynolds, D. N. (2011) *Current Microbiology* **63**, 439-449

40. Ram, J. L., Ritchie, R. P., Fang, J., Gonzalez, F. S., and Selegean, J. P. (2004) *Journal of Environmental Quality* **33**, 1024-1032

41. Clermont, O., Bonacorsi, S., and Bingen, E. (2000) *Applied and Environmental Microbiology* **66**, 4555-4558

42. Higgins, J., Hohn, C., Hornor, S., Frana, M., Denver, M., and Joerger, R. (2007) *Journal of Microbiological Methods* **70**, 227-235

43. Yang, H.-H., Vinopal, R. T., Grasso, D., and Smets, B. F. (2004) *Appl. Environ. Microbiol.* **70**, 1528-1536

44. EPA, U. S. (1994) Synthetic Precipitation Leaching Procedure. in *EPA Method 1312* (NCEP ed., 3rd Ed., Cincinnati, OH

45. Azeredo, J., and Oliveira, R. (1996) *Biotechnology Techniques* **10**, 341-344

46. Switzer, R., and Garrity, L. (1999) *Experimental Biochemistry*, W.H. Freeman Publishing

47. Dubois, M., Gilles, K. A., Hamilton, J. K., Rebers, P. A., and Smith, F. (1956) *Analytical Chemistry* **28**, 350-356

48. O'Brien, R. W., and White, L. R. (1978) *Journal of the Chemical Society, Faraday Transactions 2: Molecular and Chemical Physics* **74**, 1607-1626

49. Pembrey, R. S., Marshall, K. C., and Schneider, R. P. (1999) *Appl. Environ. Microbiol.* **65**, 2877-2894

50. Walker, S. L. (2005) *Colloids and Surfaces B: Biointerfaces* **45**, 181-188

51. Bolster, C. H., Hornberger, G. M., Mills, A. L., and Wilson, J. L. (1998) *Environmental Science & Technology* **32**, 1329-1332

52. Ma, H., Pedel, J., Fife, P., and Johnson, W. P. (2009) *Environmental Science & Technology* **43**, 8573-8579

53. Redman, J. A., Walker, S. L., and Elimelech, M. (2004) *Environmental Science & Technology* **38**, 1777-1785

54. Elimelech, M., Gregory, J., Jia, X., and Williams, R. A. (1995) *Particle Deposition and Aggregation*

Chapter 4

Linking Microbial Community Structure to Function in Representative Simulated Systems

Marcus, I. M.; Wilder, H. A.; Quazi, S. J.; Walker, S. L. 2013. Linking Microbial Community Structure to Function in Representative Simulated Systems. *Applied and Environmental Microbiology*. DOI: 10.1128/AEM.03461-12.

Abstract

Pathogenic bacteria are generally studied as a single strain under ideal growing conditions, though these conditions are not the norm in the environments in which pathogens typically proliferate. In this investigation a representative microbial community along with *Escherichia coli* O157:H7, a model pathogen, were studied in three environments in which such a pathogen could be found: a human colon, septic tank, and groundwater. Each of these systems were built in the lab to retain the physical/chemical and microbial complexity of the environments, while maintaining control of the feed into the models. The microbial community in the colon was found to have a high percentage of bacteriodetes and firmicutes, while the septic tank and groundwater systems were composed mostly of proteobacteria. The introduction of *E. coli* O157:H7 into the simulated systems elicited a shift in the structure and phenotypic cell characteristics of the microbial community. The fate and transport of the microbial community with *E. coli* O157:H7 were found to be significantly different than *E. coli* O157:H7 studied as a single isolate, suggesting an altered behavior of the organism in the environment than previously conceived. The findings in this study clearly suggest that to gain insight into the fate of pathogens, cells should be grown and analyzed under conditions simulating the environment in which the pathogens are present.

4.1 Introduction

The common paradigm when studying pathogenic bacteria in the lab has been to grow the cells as a single strain in rich nutrient media and then to harvest and evaluate the organisms' phenotypic and/or genotypic characteristics (1). However, this traditional approach overlooks a critical fact that these pathogens do not exist in such idealized conditions (2). Microorganisms survive in complex communities of multiple species of bacteria, archaea, fungi, and protozoa, albeit bacteria make up most of the biomass (3-5). It is therefore imperative to study the microbial community as a biological system and to establish the pathogen's effect on the microbial community in the environment.

One method which avoids the short comings of studying individual microorganisms is to sample bacteria directly from the environment under investigation. This approach allows for the study of microorganisms in their natural environmental settings and has produced a wealth of data on microbial communities in the human microbiome (6-10) and in aquatic systems (11-14). However, there is no realistic capacity to control parameters within *in vivo* systems. *In vitro* systems, on the other hand, combine the complexity of the environmental conditions while ensuring proper controls in the laboratory. There have been several *in vitro* models that have been developed to simulate environments where pathogens may be found including the gut of humans (15-17) and synthetic aquatic systems (18-20). These *in vitro* studies have allowed for researchers to

gain a better understanding of the behavior of microorganisms in environmentally relevant systems.

The function of *in vitro* gut environments has been tested by determining the microorganisms present (17, 21-23), by monitoring fatty-acid production (15, 17, 21, 24), and enzymatic activity (17, 21). For aquatic systems such as surface water, wastewater, and groundwater, researchers generally have used synthetic formulas to recreate the aquatic chemistry found in those environments to alleviate variability (18, 25-28). These *in vitro* environments have never been combined to study the life cycle of microbial communities from the human colon to water treatment to groundwater.

Therefore three simulated environments, a human descending colon, a two-chambered septic tank, and a groundwater system, were built to determine how microorganisms change depending on varying the *in vivo* conditions. These systems were chosen because they represent a pathway in which pathogens may be transported from a human host into groundwater. The aims of this study were to simulate environmentally relevant systems in the lab, to evaluate the structure and function of the microbial community present in each of these systems, and to evaluate those same characteristics with the addition of *Escherichia coli* O157:H7.

4.2 Materials and Methods

4.2.1 Bacterial cell and media selection

Escherichia coli O157:H7 (EDL933) was acquired from the USDA (Mark Ibekwe, USDA-ARS-USSL, Riverside, CA) for use as the model enteric pathogen in this study. The microbial community was taken from human fecal material donated by a healthy 25 year old male volunteer, who had not had antibiotics for a year. The sample used in the model colon was separated from the fecal matter using a five-cycle differential centrifugation process and stored in glycerol stocks in a -80 ºC freezer (Revco Plus, Thermo Scientific, Asheville, NC) as described previously (29). Briefly, 10 g of fecal matter were placed in 200 mL of 50 mM sodium phosphate buffer. After shaking, the sample was centrifuged at 200 x *g* for 15 minutes (Eppendorf 5804R, Hamburg, Germany). The supernatant was placed in a clean flask and kept on ice while the pellet was again transferred to the buffer, resuspended, and the process was repeated four more times. The bacteria in the supernatant were then extracted by centrifuging at 3700 x *g* for 15 minutes and suspending the pelleted bacteria in 5 mL of previously autoclaved media. This medium is similar in composition to digested food entering the large intestine (colon media) (30) and contains per liter: 4.5 g NaCl, 2.5 g K_2HPO_4, 0.45 g $CaCl_2 \cdot 2H_2O$, 0.5 g $MgSO_4 \cdot 7H_2O$, 0.005 g $FeSO_4 \cdot 7H_2O$, 0.05 g ox bile, 0.01 g haemin, 0.4 g cystein, 0.6 g pectin, 0.6 g xylan, 0.6 g arabinogalactan, 0.6 g amylopectin, 5 g starch, 2 mL Tween 80, 3 g bactopeptone, and 3 g casein. Additionally 1 mL of a vitamin mixture containing per liter was added after autoclaving: 1 mg menadione, 2 mg D-biotin, 0.5 mg vitamin B-12,

10 mg pantothenate, 5 mg nico-tinamide, 5 mg para-aminobenzoic acid, and 4 mg thiamine. The cells suspended in the media were allowed to grow in a shaker-incubator (200 rpm and 37 ºC) (Barnstead Lab-line 4639, Rose Park, Il) for 12 hr. Subsequently, 2 mL were transferred to 200 mL of the same autoclaved media and allowed to grow for 6 hr. Next 500 µL of cells were added to 500 µL of a 50% glycerol solution and stored in the -80 ºC freezer until future use. All chemicals utilized were ACS research grade.

***In vitro* human colon.** A human colon was simulated by a custom reactor maintained at pH 5.5 and 37 ºC within an incubator (Barnstead MaxQ 4000, Thermo Scientific, Asheville, NC), since these are the conditions of the proximal colon (31). The model consists of a 50 cm-long glass tube with a 5 cm internal diameter, a rubber stopper at both ends, and an internal tube sustaining a cylindrically shaped dialysis membrane 3.3 cm in diameter (diameter 33 mm, pore size 12,000 Da, Fisherbrand, Pittsburgh, PA) (Figure 4.1).

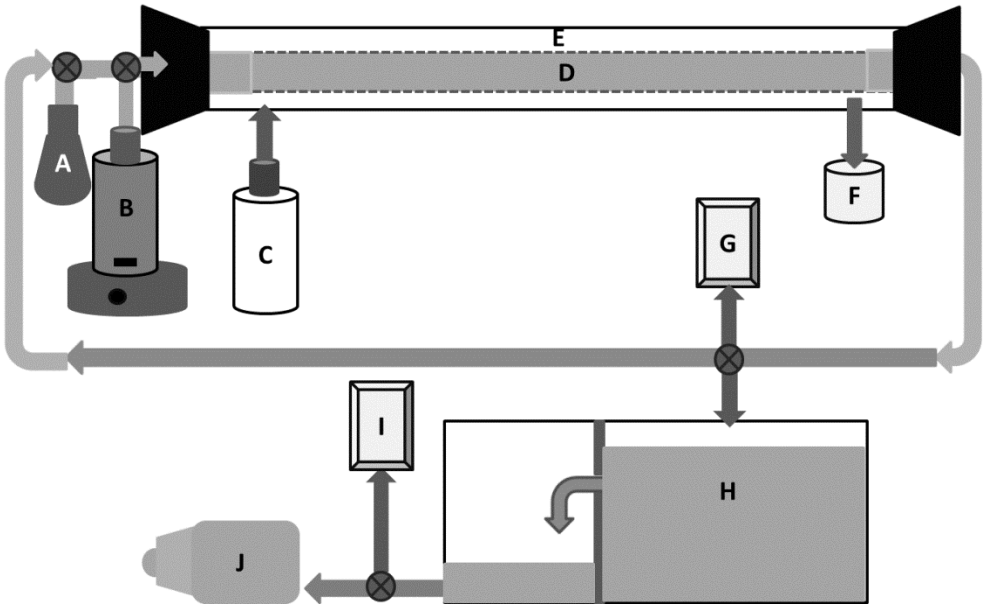

Figure 4.1. Schematic and flow diagram of the experimental apparatus and design. (A) Microbial community (and E. coli O157:H7 in select experiments), (B) colon media, (C) PEG, (D) dialysis tubing (location microbial community is inoculated), (E) PEG flows between reactor wall and dialysis tube, (F) PEG tested for fatty acids, (G) cells taken out for characterization, (H) two-chamber septic tank inoculated with the colon effluent, (I) cells taken out for characterization, and (J) groundwater inoculated from effluent from septic tank and characterized.

Each colon experiment lasted for one week. At the beginning of each week the microbial community was taken from the stored glycerol stocks and inoculated in 200 mL colon media (27) and placed in a shaker-incubator at 200 rpm and a temperature of 37 ºC for 24 hr. The bacteria suspension was then pumped into the dialysis tube of the model colon (Figure 4.1D) at a rate of 5 mL/min (Masterflex, Cole Parmer, Il) (15) (Figure 1A). A polyethylene glycol (PEG) mix was used to simulate the intestinal adsorption acting as a dehydrating medium with a per liter mixture of 26.25 g polyethylene glycol 4000, 0.36 g $NaHCO_3$ and 0.7 g NaCl (15) (Figure 4.1C). This was

fed simultaneously into the area between the dialysis and glass tubing in the model colon at a rate of 2.1 mL/min (Figure 4.1E) before flowing the bacteria and media into the model, and continuously until the end of the experiment as described in previous research (15). To simulate typical adult feeding times, 100 mL of the colon media mixture was pumped into the dialysis tube three times a day at a rate of 5 mL/min, 6 hr apart (15) (Figure 4.1D). This weeklong experiment was repeated three times to ensure reproducibility.

Subsequently, three experiments were conducted in which the microbial community was spiked at a 1:1000 ratio by volume with the model pathogen and inoculated in the model colon reactor. In these experiments a single colony of *E. coli* O157:H7 was aseptically picked from a plate, put into a 5 mL colon media mixture, and shaken in a shaker-incubator (200 rpm and 37 ºC). After 16 hr, 200 µl of the *E. coli* O157:H7 suspension was added to the 200 mL microbial community culture before inoculating the model. The rest of the experiment was operated in the same fashion as stated in the previous paragraph.

4.2.2 Short-chain fatty acid analysis

Effluent from the model colon (Figure 4.1F) and PEG solution (Figure 4.1E) were sampled at each feeding time and stored at -20 ºC until analysis. The short chain fatty acids (SCFAs), butyric acid, propionic acid, and acetic acid were detected by Gas-Liquid Chromatography (GC) (Agilent, Santa Clara, CA) using previously published methods

(28) with the detector temperature set to 200 ºC. SCFAs were measured by integrating under a fitted flame ionization detection curve.

4.2.3 Laboratory scale septic tank

About 20% of all American households (26 million) and 25% of planned developments use septic tanks to dispose of their wastewater (29). These are generally self-regulated with each State having distinct maintenance standards. It is for these reasons that a septic tank was modeled. The septic system was made by compartmentalizing an acrylic fish tank as a scaled down version of a two-compartment septic tank (144 and 72 L) with a 2:1 volume (30) (Figure 4.1H). The 100 mL of effluent collected from the colon was diluted by deionized water (DI) at a 17.5:1 ratio (1.75 L) to simulate toilet flushing. The diluted colon effluent was poured into the first compartment of the model septic tank along with synthetic greywater (3.5 L) at a 1:2 volume ratio three times a day. This ratio was selected as approximately two thirds of household wastewater comes from sources other than the toilet flushing (31). The synthetic greywater on a per liter basis is composed of 20 mg humic acid, 50 mg kaolin, 50 mg cellulose, 0.5 mM $CaCl_2$, 10 mM NaCl, and 1 mM $NaHCO_3$ at pH 8 (24). The septic water was transferred from the first partition into the second compartment once the water reached 80% of the septic tank's height (64 cm), which equated to a three week residence time in the first compartment.

Water quality tests on the model septic tank were conducted once per week to ensure the water quality was similar to that of a full-scale functioning septic system (31)

(Figure 4.1I). These tests include pH, conductivity, hardness, total organic carbon (TOC) and total suspended solids (TSS). Conductivity and pH were measured using a conductivity probe (3200 Conductivity Instrument, YSI, Yellow Springs, OH) and a pH probe (XL15, Fisher Scientific, Pittsburgh, PA), respectively. A colorimetric titration was used to determine a hardness value (32). TOC was measured using a TOC analyzer (TOC 5050, Shimadzu, Japan) (32). While TSS was measured by using a vacuum to force the water sample through a previously weighed 0.45 μm glass fiber filter. After drying the filter at 105 ºC in an oven, the filter was weighed again to quantify the amount of TSS (32).

4.2.4 Simulating groundwater conditions

Samples from the second compartment of the septic tank (900 mL) were centrifuged at 3700 x *g* and the pelleted bacteria were resuspended in 900 mL of synthetic groundwater (33,34). The resuspended bacteria were placed in two 500 mL tissue culture flasks wrapped in aluminum foil to limit light exposure and shaken at 70 rpm at room temperature as done in previous research (18) (Figure 4.1J).

4.2.5 Pyrosequencing

In order to determine the structure of the microbial community in each of the simulated systems, DNA was extracted from the samples using the MO-BIO total microbial DNA extraction kit (Carlsbad, CA) according to the manufacturer's protocol with one exception. The protocol calls for 1 mL of sample, however this would yield too

small of a quantity of DNA from the septic tank and groundwater samples. Therefore, 300 mL samples from the septic tank and groundwater systems were first centrifuged at 3700 x *g* and resuspended in 3 mL of 10 mM KCl solution before extracting the DNA. These DNA samples were then shipped to the Research and Testing Laboratory (Lubbock, TX) for bacterial tag-encoded FLX amplicon pyrosequencing (bTEFAP) using Gray28F 5' GAGTTTGATCNTGGCTCAG and Gray519r 5' GTNTTACNGCGGCKGCTG (35). The Roche 454 FLX instrument with titanium reagents and procedures were based upon the manufacturer's protocols (www.researchandtesting.com). QIIME (Quantitative Insights Into Microbial Ecology) software (36) was used to analyze the sequences. The sequences were first de-noised, assigned operational taxonomic units with a 97% pairwise identity threshold, and finally allotted taxonomic identities.

4.2.6 Microbial community phenotypic characterization

The phenotypic characterization conducted included: hydrophobicity, electrophoretic mobility, cell size, extracellular polymeric substance content and composition, and calculation of the attachment efficiency of the entire microbial community through porous media. At a consistent time each week a sample was taken from the colon, septic tank, and groundwater systems. The bacteria from the systems (colon effluent, second compartment of the septic tank, and post groundwater exposure) were washed via centrifugation (3700 x *g*) and suspended in a 10 mM potassium chloride (KCl).

Hydrophobicity was measured by the microbial adhesion to hydrocarbon (MATH) test, which gives a quantitative measure of the amount of cells partitioning in the hydrocarbon versus the electrolyte phase (37). The average microbial size, notably the length, width and subsequent average equivalent spherical radius, were determined from three images ($n > 20$) utilizing a phase contrast microscope and imaging software (Matlab, Mathworks, Natick, MA) (37). Electrophoretic mobility measurements were conducted using a zeta potential analyzer (Zetapals, Brookhaven Instruments Corp., Brookhaven, NJ) (38). Extracellular polymeric substances (EPS) were quantified as total proteins and total sugars by fixing the cells in a 0.22 % formaldehyde solution, separating the cells from the EPS, lyophilizing the EPS, and measuring the sugar and protein content using previously described colorimetric methods (33). The above phenotypic measures were conducted in triplicate.

Attachment efficiency, a measure of the adhesive nature of the cells, was determined by using a 14 cm saturated column (Kimble-Chase, Vineland, NJ) packed with 275 μm spherical diameter quartz sand (Iota, Unimin Corp., New Canaan, CT). For these transport experiments, washed cells were diluted using 10 mM KCl to an optical density of 0.2 at 546 nm. The bacterial solutions were pumped into the column for 3 pore volumes (PV) followed by 5 PV of bacteria-free electrolyte solution. The effluent was measured using an in-line spectrometer at 546 nm (Turner, Barnstead International, Dubuque, Iowa) to determine the deposition of the microbial community (39) and their attachment efficiency in the column (40).

4.2.7 Statistical and data analysis

Student pair t-tests with normal distribution in Excel (Microsoft, Redmond, WA) were used to analyze the week to week variation of the structure and function of the microbial community. One-way analysis of variance (ANOVA) with normal distribution and homogeneity of variance was used to look at significance in the variances between the results from the different simulated systems. Differences were considered significant with a P value of less than 0.05.

4.3 Results and Discussion

4.3.1 Composition of microbial community (phylum)

Samples were taken from the colon, septic tank, and groundwater systems to analyze the microbial communities' structure, fate, and transport at the same time once per week to ensure reproducibility. The microbial communities' structure was analyzed with pyrosequencing and in the analysis the following measures were taken to enhance the comparability of amplicon sequencing data: removal of all singletons rare operational taxonomic units (OTUs), as well as adding sequences from technical replicate sequencing runs. For the first three weeks of experiments the microbial community was tested without *E. coli* O157:H7. The following three weeks the model pathogen was introduced into the colon and subsequently added to the aquatic systems. The result of the microbial community structure analysis at the phylum level is displayed in Figure 4.2. The model colon had a composition that was within the normal range according to Arumugam et al.

(7), where the community was composed of mostly firmicutes and bacteriodetes. In the *in vitro* colon, the microbial community without the pathogen was composed of mostly bacteriodetes (94 ± 2 %), firmicutes (5 ± 3 %), and proteobacteria (0.8 ± 0.6 %). The same did not hold true for the community with the pathogen, as the relative amount of firmicutes and actinobacteria increased (74 ± 18 % and 4 ± 2 %, respectively) at the expense of the bacteriodetes (20 ± 17 %). Meanwhile, the relative amount of proteobacteria remained consistent (1.5 ± 0.8 %). The relative amount of proteobacteria was comparable in the septic tank (85 ± 5 %) and groundwater system (83 ± 5 %) without the pathogen ($P > 0.05$). The similarity between the aquatic systems for the relative amount of proteobacteria held true for the septic tank (60 ± 9 %) and groundwater (56 ± 3 %) with the pathogen ($P > 0.05$). Though the relative quantity of proteobacteria dominated the bacterial composition in both aquatic systems there was a significant difference ($P < 0.05$) between the experiments without and with the pathogen. In the septic tank, the relative amount of bacteriodetes was higher with the pathogen (25 ± 4 %) than without (3 ± 1 %), while the relative amount of firmicutes was relatively consistent (15 ± 4 % with the pathogen and 13 ± 4 % without). The opposite trend was true for the groundwater system, with the relative amount of firmicutes being greater with (26 ± 7 %) than without the pathogen (7 ± 6 %), while the relative amount of bacteriodetes was consistent (18 ± 5 % with and 11 ± 11 % without).

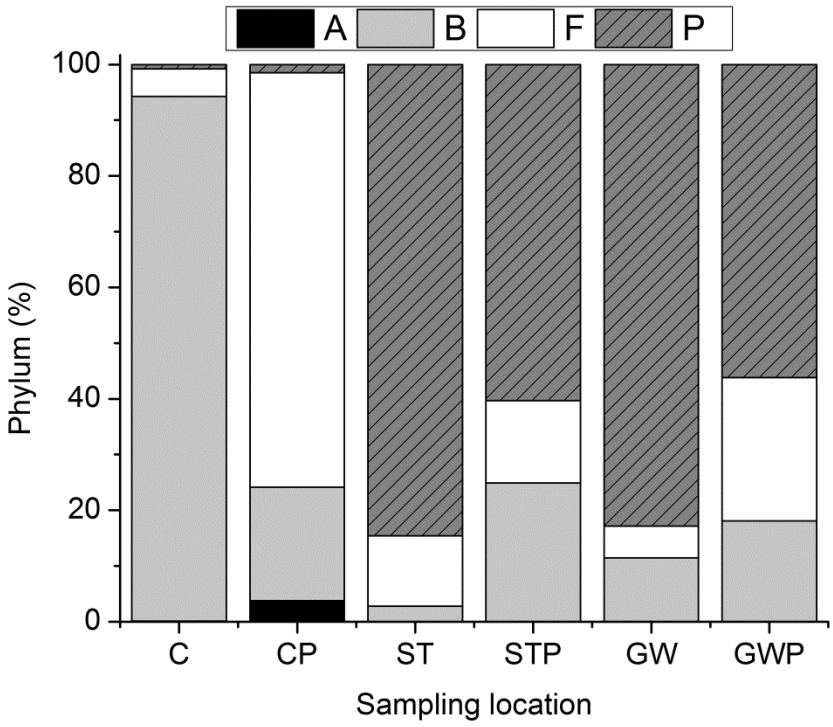

Figure 4.2. The average percentage of the four most prominent bacterial phylums (A=Actinobacteria, P=Proteobacteria, F=Firmicutes, and B=Bacteriodetes) in each of the model systems (C=Colon, CP=Colon with model pathogen, ST=Septic tank, STP= Septic tank with model pathogen, GW=Groundwater, and GWP= Groundwater with model pathogen).

4.3.2 Microbial community activity in the model colon

The composition of short-chain fatty acids was relatively consistent in the colon environment over time (Figure 4.3). Without *E. coli* O157:H7 present the acetic/butyric/propionic composition ratio was 5/4/1. When the pathogen was introduced into the microbial community the acetic/ butyric/propionic ratio changed to 2/6/2. In both cases propionic acid was the lowest, whereas acetic acid decreased and butyric acid

increased with *E. coli* O157:H7 present. These datasets were significantly ($P < 0.05$) distinct from each other.

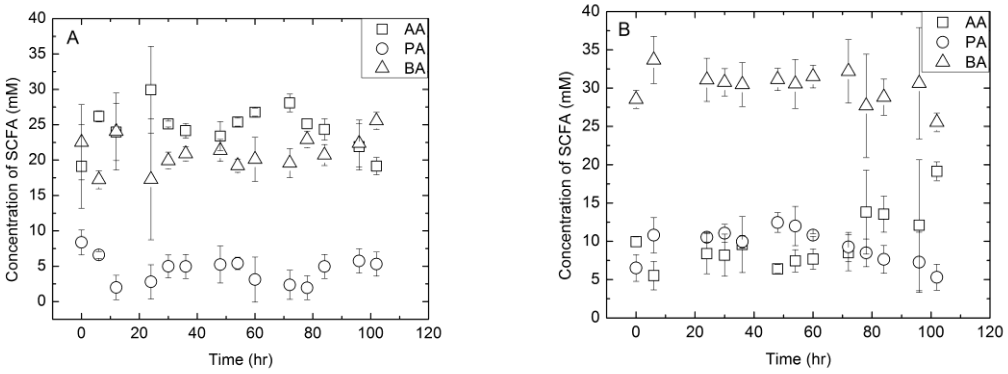

Figure 4.3. Comparison of the concentration of short-chain fatty acids (AA=Acetic acid, PA=Propionic acid, and BA=Butyric acid) over a five day period in the model colon (A) without and (B) with *E. coli* O157:H7.

4.3.3 Physical-chemical characteristics of the microbial community

The microbial community from the colon was significantly ($P < 0.05$) more hydrophilic and had lower electrophoretic mobility, attachment efficiency, and EPS content than the microbial communities harvested from the model aquatic systems (Table 4.1). With the addition of *E. coli* O157:H7, the colon's microbial community had a statistically lower ($P < 0.05$) electrophoretic mobility and attachment efficiency, and a higher sugar and protein content than the aquatic systems. There was no statistical difference between the physical-chemical characteristics of the microbial communities in the septic tank and groundwater systems in the presence and absence of *E. coli* O157:H7. The addition of the pathogen significantly ($P < 0.05$) increased the hydrophobicity and

EPS level of the bacteria grown in the colon, reduced the EPS in the aquatic systems and enlarged the average cell size in all three systems.

Table 4.1. Measured values of selected cell surface properties and the attachment efficiency of the cells in column transport experiments. Standard deviations are in parentheses. Within each column, values with the same letter are not significantly different at the P = 0.05 level.

Sample	Hydrophobicity (%)	Electrophoretic Mobility ($cm\ s^{-1}\ V^{-1}$)	Radius (μm)	EPS: Sugar ($mg/10^{10}$ cell)	EPS: Protein ($mg/10^{10}$ cell)	Attachment Efficiency
Colon	12.5a (6.5)	-1.67a (0.20)	0.46a (0.02)	6.30a (2.9)	31.1a (6.5)	0.22a (0.09)
Septic Tank	40.1b (2.8)	-1.10b (0.37)	0.51a (0.05)	15.3b (3.1)	120b (58)	0.47b (0.2)
Groundwater	55.1b (6.3)	-1.35b (0.05)	0.48a (0.03)	15.1b (6.3)	126b (29)	0.56b (0.1)
Colon w/Pathogen	36.3b (10)	-1.95a (0.25)	0.57b (0.1)	17.8b (7.9)	78.5b (26)	0.34a (0.04)
Septic Tank w/Pathogen	51.8b (8.4)	-1.24b (0.18)	0.60b (0.07)	5.15a (3.4)	47.6a (15)	0.47b (0.09)
Groundwater w/Pathogen	34.8b (9.5)	-1.38b (0.22)	0.57b (0.08)	4.69a (4.4)	44.7a (17)	0.55b (0.1)

4.3.4 Water quality of septic tank

In order to confirm that the model septic tank performed in the same way as its real world counterpart (41), standard water quality tests were performed on the effluent once per week for the seven weeks that the system was operational and compared to reported values from the literature (31). The average and standard deviation for the selected tests are displayed in Table 4.2.

Table 4.2. Water quality analysis of the model septic tank. Standard deviations are in parentheses.

Water Quality Test	Model Septic Tank
Alkalinity (mg/L as $CaCO_3$)	300 (25)
pH	6.8 (0.5)
Conductivity (µS/cm)	1.39 (.05)
TOC[1] (mg/L)	152.6 (10)
Hardness (mg/L as $CaCO_3$)	51 (5)
TSS[2] (mg/L)	28 (7)
BOD[3] (mg/L)	61 (8)
Total organisms (cells/mL)	10^6 (10^5)

[1]TOC – Total organic carbon, [2]TSS – Total suspended solids, [3]BOD – Biological oxygen demand

4.3.5 Analysis of microbial structure and SCFA analysis in colon

The microbial community within the model colon was compared to *in vitro* and *in vivo* colon environments from previous studies in terms of microbial composition using 16S based pyrosequencing. While there are known issues associated with the 16S pyrosequencing technique such as PCR bias (46), sequencing errors (47, 48), and quantification of data (49), this study followed the guidelines established in Zhou *et al*. for increasing data comparability (50). Specifically, rare OTUs and singletons were removed, three biological replicates under each condition were tested, and all samples were collected and analyzed in the same manner to ensure more reproducible data. In the absence of the pathogen the relatively high amount of bacteriodetes in the microbial community agrees with previously studied *in vitro* models (17, 23, 51, 52) and human gut microbiomes (7, 53). The majority of the real colon microbiomes have a higher concentration of firmicutes than bacteriodetes (7, 53). This microbial composition is similar to the *in vitro* colon in this study with the addition of *E. coli* O157:H7. Within a

mouse colon model the production of firmicutes was amplified with the addition of an enterohaemorrhagic *E. coli* pathogen to the microbial community in the gut (54, 55). Previous research has shown that the diversity of the indigenous microbial community is an important factor in determining whether invasive *E. coli* will be able to colonize an environment (56). It is broadly accepted in the literature that microbial communities with higher biodiversity are most resistant to changes in their structure and function than lower biodiversity (56-59). In one of these studies where *E. coli* O157:H7 changed the community structure, the researchers explained the shift by suggesting that there was limited functional redundancy (56). The lack of functional redundancy allows the pathogen to establish an ecological niche in a microbial community that lacked functional redundancy.

4.3.6 Analysis of microbial activity in colon

The microbial activity of the colon in this study was compared to previous *in vivo* and *in vitro* gut environments by quantifying the short-chain fatty acids in the model colon. The total fatty acid content in the colon was insensitive the presence or absence of the pathogen. Though, acetic acid levels decreased significantly ($P < 0.05$), while butyric acid increased significantly ($P < 0.05$) with *E. coli* O157:H7 present. Previous studies have suggested that microbial composition and fatty acid differences could be attributed to diet (15, 60-63), pH (64), peptide supply (64), and the relative amount of oxygen in the system (65, 66). However, these parameters were consistent in this study, suggesting the

altered community structure is impacting the fatty acid composition of the model colon (64, 67). Previous research has shown that acetic acid impairs *E. coli* O157:H7 in the gut (68), *while* the introduction of *E. coli* O157:H7 could increase the relative amount of butyric acid (69). This would enhance the production of virulence genes allowing the pathogen to establish a niche in the colon. An established microbial community may be robust enough to negate the effects of *E. coli* O157:H7 on microbial community structure by increasing the production of acetic acid while reducing butyric acid (24). The shift in short-chain fatty acid production in this study implies that the pathogen is now fully integrated into the microbial community and influencing the behavior of the microbial community to reduce acetate production and increase butyric acid production in order to produce virulence factors and find an ecological niche.

4.3.7 Microbial community structure in aquatic systems

The microbial structure and water quality were assessed for the aquatic systems to ensure that they accurately represented the simulated environments. The septic tank was inoculated with the microbial community from the model colon, yet the composition varied greatly from the inoculum. Previous research has shown that proteobacteria tends to survive and thrive better than bacteriodetes and firmicutes in domestic wastewater systems (55), which is similar to this model septic system. Not only was the microbial data similar to that of an actual wastewater system, but all of the water quality values of the model septic tank fell into the range of a real septic tank process (31). Regardless of

pathogen presence, the microbial community composition of the groundwater samples were mostly composed of proteobacteria, with a higher percentage of firmicutes and bacteriodetes than the model septic tank effluent. The structure of the microbial community in the groundwater experiments was similar to previous research where groundwater was contaminated from livestock wastewater (56) and other perturbed environmental conditions (11).

4.3.8 Microbial community phenotypic analysis

The following extensive phenotypic cell characterizations tested: hydrophobicity, EPM, radius, EPS content, and attachment efficiency were chosen since they have been linked to the fate and transport of microorganisms in the environment (42, 72-74) and can be used for comparative evaluation between different environmental microbial communities. In the absence of *E. coli* O157:H7, cells from the colon had lower hydrophobicity, EPM, EPS, and attachment efficiency values than the microbial communities in the aquatic systems. In the presence of the *E. coli* O157:H7 the change in community structure lead to some significant alterations in the microbial community's phenotypic response. In the colon the change in community structure led to an increase in hydrophobicity, which has been shown to affect microbial deposition on to surfaces and the formation of biofilms (75, 76). The perturbation also changed the quantities of EPS in all systems, with an increase in production with *E. coli* present in the colon, but a decrease in the aquatic systems. This may make the microbial community less likely to

attach to surfaces to form biofilms in aquatic systems. The average size of the microbial community significantly increased in all three systems when *E. coli* O157:H7 was present, which could affect the community's transport through porous media.

There were a few statistically significant correlations between the cell properties of the three environmental systems. Similar to previous work using regression analysis, the attachment efficiency was found to be correlated to the electrophoretic mobility (57-59) and hydrophobicity (63). Additionally, the attachment efficiency was inversely proportional to the EPS sugar to protein ratio ($P < 0.05$) (59). These relationships show that the cell surface characterization (hydrophobicity, EPM, and EPS ratio) of the heterogeneous microbial community can be correlated to the transport properties (attachment efficiency) of the cells in all of these representative systems.

4.3.8 Microbial community phenotypic comparison to isolated *E. coli* O157:H7

In order to better explain the impact of the microbial community in the three model systems (colon, septic tank, and groundwater) on *E. coli* O157:H7, a comparison was made between the results in this study and that of *E. coli* O157:H7 grown in idealized lab conditions. The results from Haznedaroglu et al. (2009), a study which investigated the fate and transport of *E. coli* O157:H7 and Salmonella SA1685 under idealized conditions (10 mM KCl, the same ionic strength and salt condition used for cell phenotypic analysis in this current work) (77). This comparison can provide indirect

insight of the impact the microbial community has on *E. coli* by comparing the bacteria's condition grown in the presence and absence of a microbial community. The hydrophobicity of E. coli in the Haznedaroglu study was significantly lower (19 ± 2 %) than that of the *E. coli* evaluated along with the microbial community (35-52 %) from each of the model systems. This increase in hydrophobicity for *E. coli* within a microbial community versus the isolate may further impact the fate of the cell, as hydrophobic interactions have been shown to affect microbial deposition on surfaces and to influence the formation of biofilms (75, 76). Another phenotypic measure of the isolate versus microbial community grown *E. coli* O157:H7 is the electrophoretic mobility (EPM), which has been linked to the stability and attachment of bacteria. Notably, higher absolute values of EPM correlate to more stable organisms (78, 79). The EPM for the individual isolate in the Haznedaroglu study was much less negatively charged (-0.14 $Vs^{-1}cm^{-1}$) (77) than that measured for *E. coli* O157:H7 with the microbial community (-1.95 – -1.24 $Vs^{-1}cm^{-1}$)**.** This suggests that the microbial community of which *E. coli* is a part in this current study will be more stable in suspension than the individual isolate. Next, the extracellular polymer substance (EPS) content was evaluated via the sugar/protein ratio to compare between the individually grown *E. coli* isolate vs. that grown in the community. The EPS sugar and protein content was evaluated as they have been reported as an indicator of cell condition (80). It was observed that the sugar/protein ratio was greatly enhanced with the microbial community present (0.10-0.23) as compared to *E. coli* O157:H7 in the Haznedaroglu study (0.03). The increase in sugar relative to protein in the EPS has been previously related to biofilm formation (81), suggesting that the *E.*

coli within the microbial community has a higher likelihood of being part of a biofilm than isolated *E. coli* O157:H7.

The surface charge of the bacteria, as enumerated by EPM, suggest that the *E. coli* in the microbial community is more stable and would be more mobile than the *E. coli* isolate alone (as in the Haznedaroglu study). However, the hydrophobicity and EPS analysis suggests that there are substantial hydrophobic interactions at play in the presence of the microbial community that may lead to greater attachment of the cells. The impact of these mechanisms can be compared in the transport data. The Haznedaroglu study did not report attachment efficiency, but rather used deposition rates to predict the transport distance at which 3 log removal (99.9%) of the *E. coli* would be achieved flowing in porous media (82-84). This is a method commonly used to assess fate and transport (85, 86). Haznedaroglu *et al*. found that isolated *E. coli* O157:H7 could travel 3.7 meters before removal of 99.9 % of the cells. Similar calculations were conducted on the microbial consortia with *E. coli* O157:H7, which consistently required a shorter distance to achieve 3 log removal. This suggests that the cells in the microbial community are much more adhesive than the *E. coli* isolate alone. Based on this study, 0.1% of the *E. coli* has the potential of traveling beyond 1.4 meters, 0.9 m, and 0.8 m if released into the groundwater environment directly from the model colon, septic tank, and synthetic groundwater system, respectively. These calculations suggest that *E. coli* is impacted by the presence of a microbial community in that it becomes less likely to be

transported in the subsurface, as opposed to an isolated cell without the complexity of the consortium.

4.4 Conclusions

In this study three *in vitro* systems were developed to replicate representative environmental conditions. These *in vitro* systems successfully simulated the community structure and function of their *in vivo* counterparts. This approach has allowed for the investigation of the microbial community's response to the introduction of *E. coli* O157:H7. The differences described here (hydrophobicity, electrophoretic mobility, EPS levels, and general transport calculations) suggest that *E. coli* O157:H7 within a microbial community may be less mobile in aquatic environments and more prone to biofilm formation than the isolated strain. This study is an initial step in understanding how microbial communities behave in the environment and how resilient the structure and function of the consortia are to the introduction of invasive species. Other pathogenic bacteria may have a different effect on native microbial communities. Thus, more research is needed to determine the long-term effects of pathogens in the microbial community in complex environments.

4.5 References

1. Madigan, M. T., Martinko, J.M. (2006) *Biology of Microorganisms*, 11th ed., Pearson Prentice Hall, Upper Saddle River, N.J.
2. R.R. Colwell, D. J. G. (2000) *Nonculturable microorganisms in the environment*, ASM Press
3. Buée, M., De Boer, W., Martin, F., van Overbeek, L., and Jurkevitch, E. (2009) *Plant and Soil* **321**, 189-212
4. Wegley, L., Edwards, R., Rodriguez-Brito, B., Liu, H., and Rohwer, F. (2007) *Environmental Microbiology* **9**, 2707-2719
5. Benckiser, G., and Bamforth, S. (2011) *Agronomy for Sustainable Development* **31**, 205-215
6. Duytschaever, G., Huys, G., Bekaert, M., Boulanger, L., De Boeck, K., and Vandamme, P. (2011) *Appl. Environ. Microbiol.* **77**, 8015-8024
7. Arumugam, M., Raes, J., Pelletier, E., Le Paslier, D., Yamada, T., Mende, D. R., Fernandes, G. R., Tap, J., Bruls, T., Batto, J.-M., Bertalan, M., Borruel, N., Casellas, F., Fernandez, L., Gautier, L., Hansen, T., Hattori, M., Hayashi, T., Kleerebezem, M., Kurokawa, K., Leclerc, M., Levenez, F., Manichanh, C., Nielsen, H. B., Nielsen, T., Pons, N., Poulain, J., Qin, J., Sicheritz-Ponten, T., Tims, S., Torrents, D., Ugarte, E., Zoetendal, E. G., Wang, J., Guarner, F., Pedersen, O., de Vos, W. M., Brunak, S., Dore, J., Weissenbach, J., Ehrlich, S. D., and Bork, P. (2011) *Nature* **473**, 174-180

8. Gill, S. R., Pop, M., DeBoy, R. T., Eckburg, P. B., Turnbaugh, P. J., Samuel, B. S., Gordon, J. I., Relman, D. A., Fraser-Liggett, C. M., and Nelson, K. E. (2006) *Science* **312**, 1355-1359

9. Eckburg, P. B., Bik, E. M., Bernstein, C. N., Purdom, E., Dethlefsen, L., Sargent, M., Gill, S. R., Nelson, K. E., and Relman, D. A. (2005) *Science* **308**, 1635-1638

10. Li, M., Wang, B., Zhang, M., Rantalainen, M., Wang, S., Zhou, H., Zhang, Y., Shen, J., Pang, X., Zhang, M., Wei, H., Chen, Y., Lu, H., Zuo, J., Su, M., Qiu, Y., Jia, W., Xiao, C., Smith, L. M., Yang, S., Holmes, E., Tang, H., Zhao, G., Nicholson, J. K., Li, L., and Zhao, L. (2008) *Proceedings of the National Academy of Sciences* **105**, 2117-2122

11. Griebler, C., and Lueders, T. (2009) *Freshwater Biology* **54**, 649-677

12. Tringe, S. G., von Mering, C., Kobayashi, A., Salamov, A. A., Chen, K., Chang, H. W., Podar, M., Short, J. M., Mathur, E. J., Detter, J. C., Bork, P., Hugenholtz, P., and Rubin, E. M. (2005) *Science* **308**, 554-557

13. Smith, R. J., Jeffries, T. C., Roudnew, B., Fitch, A. J., Seymour, J. R., Delpin, M. W., Newton, K., Brown, M. H., and Mitchell, J. G. (2012) *Environmental Microbiology* **14**, 240-253

14. Oh, S., Caro-Quintero, A., Tsementzi, D., DeLeon-Rodriguez, N., Luo, C., Poretsky, R., and Konstantinidis, K. T. (2011) *Appl. Environ. Microbiol.* **77**, 6000-6011

15. Jiménez-Vera, R., Monroy, O., Corona-Cruz, A., and García-Garibay, M. (2008) *World Journal of Microbiology and Biotechnology* **24**, 2767-2774

16. Macfarlane, G. T., Macfarlane, S., and Gibson, G. R. (1998) *Microbial Ecology* **35**, 180-187

17. Van den Abbeele, P., Grootaert, C., Marzorati, M., Possemiers, S., Verstraete, W., Gérard, P., Rabot, S., Bruneau, A., El Aidy, S., Derrien, M., Zoetendal, E., Kleerebezem, M., Smidt, H., and Van de Wiele, T. (2010) *Appl. Environ. Microbiol.* **76**, 5237-5246

18. Haznedaroglu, B. Z., Yates, M. V., Maduro, M. F., and Walker, S. L. (2012) *Journal of Environmental Monitoring* **14**, 41-47

19. Ghaniyari-Benis, S., Borja, R., Monemian, S. A., and Goodarzi, V. (2009) *Bioresource Technology* **100**, 1740-1745

20. Ho, J., and Sung, S. (2010) *Bioresource Technology* **101**, 2191-2196

21. Maathuis, A. J. H., van den Heuvel, E. G., Schoterman, M. H. C., and Venema, K. (2012) *The Journal of Nutrition* **142**, 1205-1212

22. van der Werf, M. J., and Venema, K. (2000) *Journal of Agricultural and Food Chemistry* **49**, 378-383

23. Rajilić-Stojanović, M., Maathuis, A., Heilig, H. G. H. J., Venema, K., de Vos, W. M., and Smidt, H. (2010) *Microbiology* **156**, 3270-3281

24. Thévenot, J., Etienne-Mesmin, L., Denis, S., Chalancon, S., Alric, M., Livrelli, V., and Blanquet-Diot, S. (2013) *Appl. Environ. Microbiol.* **79**, 1058-1064

25. Jones, T. E. (1982) Reference material chemistry: synthetic groundwater formulation.

26. Onkal Engin, G., Sinmaz Ucar, B., and Senturk, E. (2011) *Desalination and Water Treatment* **29**, 103-109

27. Nghiema, L. D., N. Oschmanna, A.I. Schäfer. (2006) *Desalination* **187**, 283-290

28. Ottofuelling, S., Von Der Kammer, F., and Hofmann, T. (2011) *Environmental Science & Technology* **45**, 10045-10052

29. Apajalahti, J. H. A., Sarkilahti, L. K., Maki, B. R. E., Heikkinen, J. P., Nurminen, P. H., and Holben, W. E. (1998) *Appl. Environ. Microbiol.* **64**, 4084-4088

30. Minekus, M., Smeets-Peeters, M., Bernalier, A., Marol-Bonnin, S., Havenaar, R., Marteau, P., Alric, M., Fonty, G., and Huis in't Veld, J. H. J. (1999) *Applied Microbiology and Biotechnology* **53**, 108-114

31. NUGENT, S. G., KUMAR, D., RAMPTON, D. S., and EVANS, D. F. (2001) *Gut* **48**, 571-577

32. Venema, K., M.H.M.C. van Nuenen, E. G. van den Heuvel, W. Pool, and J. M.B.M. van der Vossen. (2003) *Microbial Ecology in Health and Disease* **15**, 94-105

33. EPA, U. S. (2011) Decentralized Wastewater Treatment Systems: Memorandum of Understanding. (Management, O. o. W. ed., 3 Ed.

34. EPA, U. S. (1980) Onsite Wastewater Treatment and Disposal Systems. (Operations, O. o. W. P. ed., 1st Ed., Washington D.C.

35. Brandes, M. (1978) *Journal Water Pollution Control Federation* **50**, 2547-2559

36. Clesceri, L. S. G., A.E; Tussell, R.R. (ed) (1989) *Standard Methods for the Examination of Water and Wastewater*, American Public Health Association, Baltimore, MD

37. Gong, A. S., C.H. Bolster, M. Benavides, and S.L. Walker. (2009) *Environmental Engineering Science* **26**, 1523-1532

38. Bolster, C. H., Mills, A. L., Hornberger, G. M., and Herman, J. S. (1999) *Water Resour. Res.* **35**, 1797-1807

39. Dowd, S. E., T. R. Callaway, et al. (2008) *BMC Microbiol* **8**

40. Caporaso, J. G., J. Kuczynski, et al. (2010) *Nature Methods* **7**, 335-336

41. Walker, S. L., Hill, J. E., Redman, J. A., and Elimelech, M. (2005) *Appl. Environ. Microbiol.* **71**, 3093-3099

42. Tazehkand, S. S., Torkzaban, S., Bradford, S. A., and Walker, S. L. (2008) *J Environ Qual* **37**, 2108-2115

43. Kim, H. N., and Walker, S. L. (2009) *Colloids and Surfaces B: Biointerfaces* **71**, 160-167

44. Redman, J. A., Walker, S. L., and Elimelech, M. (2004) *Environmental Science & Technology* **38**, 1777-1785

45. Canter, L. W., Knox, R.C. (ed) (1985) *Septic Tanks System Effects on Groundwater Quality*, Lewis Publishers, Chelsea, Michigan

46. Pinto, A. J., and Raskin, L. (2012) *PLoS ONE* **7**, e43093

47. Quince, C., Lanzen, A., Curtis, T. P., Davenport, R. J., Hall, N., Head, I. M., Read, L. F., and Sloan, W. T. (2009) *Nat Meth* **6**, 639-641

48. Kunin, V., Engelbrektson, A., Ochman, H., and Hugenholtz, P. (2010) *Environmental Microbiology* **12**, 118-123

49. Engelbrektson, A., Kunin, V., Wrighton, K. C., Zvenigorodsky, N., Chen, F., Ochman, H., and Hugenholtz, P. (2010) *ISME J* **4**, 642-647

50. Zhou, J., Wu, L., Deng, Y., Zhi, X., Jiang, Y.-H., Tu, Q., Xie, J., Van Nostrand, J. D., He, Z., and Yang, Y. (2011) *ISME J* **5**, 1303-1313

51. Marzorati, M., Maignien, L., Verhelst, A., Luta, G., Sinnott, R., Kerckhof, F., Boon, N., Van de Wiele, T., and Possemiers, S. *Antonie van Leeuwenhoek*, 1-12

52. Allison, C., McFarlan, C., and MacFarlane, G. T. (1989) *Appl. Environ. Microbiol.* **55**, 672-678

53. Turnbaugh, P. J., Hamady, Micah, Yatsunenko, Tanya, Cantarel, Brandi L., Duncan, Alexis, Ley, Ruth E., Sogin, Mitchell L., Jones, William J., Roe, Bruce A., Affourtit, Jason P., Egholm, Michael, Henrissat, Bernard, Heath, Andrew C., Knight, Rob, Gordon, Jeffrey I. (2009) *Nature* **457**, 480-484

54. Lupp, C., Robertson, M. L., Wickham, M. E., Sekirov, I., Champion, O. L., Gaynor, E. C., and Finlay, B. B. (2007) *Cell Host & Microbe* **2**, 119-129

55. Rawls, J. F., Mahowald, M. A., Ley, R. E., and Gordon, J. I. (2006) *Cell* **127**, 423-433

56. van Elsas, J. D., Semenov, A. V., Costa, R., and Trevors, J. T. (2011) *ISME J* **5**, 173-183

57. Tilman, D. (1997) *Ecology* **78**, 81-92

58. van Elsas, J. D., Hill, P., Chronakova, A., Grekova, M., Topalova, Y., Elhottova, D., and Kristufek, V. (2007) *ISME J* **1**, 204-214

59. Trevors, J. T. (1998) *Water, Air, & Soil Pollution* **101**, 45-67

60. Macfarlane, G. T., Gibson, G. R., and Cummings, J. H. (1992) *Journal of Applied Microbiology* **72**, 57-64

61. Cummings, J. H., Pomare, E. W., Branch, W. J., Naylor, C. P., and Macfarlane, G. T. (1987) *Gut* **28**, 1221-1227

62. Mahowald, M. A., Rey, F. E., Seedorf, H., Turnbaugh, P. J., Fulton, R. S., Wollam, A., Shah, N., Wang, C., Magrini, V., Wilson, R. K., Cantarel, B. L., Coutinho, P. M., Henrissat, B., Crock, L. W., Russell, A., Verberkmoes, N. C., Hettich, R. L., and Gordon, J. I. (2009) *Proceedings of the National Academy of Sciences*

63. Bourquin, L. D., Titgemeyer, E. C., Garleb, K. A., and Fahey, G. C. (1992) *The Journal of Nutrition* **122**, 1508-1520

64. Walker, A. W., Duncan, S. H., McWilliam Leitch, E. C., Child, M. W., and Flint, H. J. (2005) *Appl. Environ. Microbiol.* **71**, 3692-3700

65. Brioukhanov, A., and Netrusov, A. (2007) *Applied Biochemistry and Microbiology* **43**, 567-582

66. Rolfe, R. D., Hentges, D. J., Campbell, B. J., and Barrett, J. T. (1978) *Appl. Environ. Microbiol.* **36**, 306-313

67. Lin, B., Gong, J., Wang, Q., Cui, S., Yu, H., and Huang, B. (2011) *Food Hydrocolloids* **25**, 180-188

68. Fukuda, S., Toh, H., Hase, K., Oshima, K., Nakanishi, Y., Yoshimura, K., Tobe, T., Clarke, J. M., Topping, D. L., Suzuki, T., Taylor, T. D., Itoh, K., Kikuchi, J., Morita, H., Hattori, M., and Ohno, H. (2011) *Nature* **469**, 543-547

69. Nakanishi, N., Tashiro, K., Kuhara, S., Hayashi, T., Sugimoto, N., and Tobe, T. (2009) *Microbiology* **155**, 521-530

70. Tomaras, J., Sahl, J. W., Siegrist, R. L., and Spear, J. R. (2009) *Appl. Environ. Microbiol.* **75**, 3348-3351

71. Cho, J.-C., and Kim, S.-J. (2000) *Appl. Environ. Microbiol.* **66**, 956-965

72. Marcus, I. M., Bolster, C. H., Cook, K. L., Opot, S. R., and Walker, S. L. (2012) *Journal of Environmental Monitoring* **14**, 984-991

73. Bolster, C. H., Cook, K. L., Marcus, I. M., Haznedaroglu, B. Z., and Walker, S. L. (2010) *Environmental Science & Technology* **44**, 5008-5014

74. Bolster, C. H., Haznedaroglu, B. Z., and Walker, S. L. (2009) *J. Environ. Qual.* **38**, 465-472

75. Marcus, I. M., Herzberg, M., Walker, S. L., and Freger, V. (2012) *Langmuir* **28**, 6396-6402

76. Schäfer, A., Ustohal, P., Harms, H., Stauffer, F., Dracos, T., and Zehnder, A. J. B. (1998) *Journal of Contaminant Hydrology* **33**, 149-169

77. Huysman, F., and Verstraete, W. (1993) *Soil Biology and Biochemistry* **25**, 83-90

78. Haznedaroglu, B. Z., Kim, H. N., Bradford, S. A., and Walker, S. L. (2009) *Environmental Science & Technology* **43**, 1838-1844

79. Hermansson, M. (1999) *Colloids and Surfaces B: Biointerfaces* **14**, 105-119

80. Elimelech, M., Gregory, J., Jia, X., and Williams, R. A. (1995) Particle Deposition and Aggregation: Measurement, Modeling and Simulation. Butterworth-Heinemann. pp 441

81. Eboigbodin, K. E., and Biggs, C. A. (2008) *Biomacromolecules* **9**, 686-695

82. Marcotte, L., Kegelaer, G., Sandt, C., Barbeau, J., and Lafleur, M. (2007) *Analytical Biochemistry* **361**, 7-14

83. Yao, K.-M., Habibian, M. T., and O'Melia, C. R. (1971) *Environmental Science & Technology* **5**, 1105-1112

84. Rajagopalan, R., and Tien, C. (1976) *Aiche Journal* **22**, 523-533

85. Liu, Y., Yang, C.-H., and Li, J. (2007) *Environmental Science & Technology* **42**, 159-165

86. Kretzschmar, R., Borkovec, M., Grolimund, D., and Elimelech, M. (1999) Mobile Subsurface Colloids and Their Role in Contaminant Transport. in *Advances in Agronomy* (Donald, L. S. ed.), Academic Press. pp 121-193

87. Li, Q., and Logan, B. E. (1999) *Water Research* **33**, 1090-1100

Chapter 5

Summary and Conclusions

The overall goal of this doctoral work was to determine the effect the environment has on bacterial pathogens in both natural and engineered systems. Two model pathogens were used (*E. coli* O157:H7 and *P. aeruginosa* PAO1), along with 11 *E. coli* environmental isolates, and a human fecal microbial community. The fate and transport of these bacteria were investigated over a wide range of growth conditions including varying the growth time, solution chemistry, and environment. The physicochemical characteristics monitored included: hydrophobicity, zeta potential, cell size, surface charge density, and EPS production. The transport studies included the usage of a QCM-D and packed-bed columns. The presence of a microbial community on the fate and transport of pathogens was also explored in this work.

Chapter 2 highlighted the role of hydrophobicity in the adherence of cells to a surface. By varying the growth phase of *Pseudomonas aeruginosa* it was found that cells grown to mid-exponential phase were hydrophilic, while stationary cells were hydrophobic. Suspensions of these cells were introduced into the QCM-D over hydrophilic silica and hydrophobic PVDF surfaces to study the influence of hydrophobicity on the initial stages of biofilm formation. Each cell-surface combination was found to have a different mechanism of attachment based on the QCM-D data and monitoring attachment visually through a fluorescent microscope. The two major finding were that (1) regardless of cell type, the bacterial attachment on the hydrophilic surface plateaued after 30 minutes, while cells continued to attach to the hydrophobic surface and (2) hydrophobic cells formed firm, elastic bonds to the surfaces, while hydrophilic cells attached to the silica surface through viscous forces, and formed a viscoelastic bond to

the PVDF sensor. This investigation has led to the understanding that growth conditions of bacteria may significantly impact the cells' physiology, ultimately affecting the extent of transport in the environment.

In Chapter 3, the physical-chemical and transport properties of 11 environmental *E. coli* isolates were investigated under idealized laboratory growth conditions and a more representative growth solution. The "ideal" growth solution was LB media (a standard laboratory bacterial growth media) and the "real" solution was bovine manure extract simulating post-host shedding environmental conditions. The physical-chemical and transport properties varied for most of isolates between the two growth conditions, but in dissimilar ways. In general, cells had a more negative zeta potential, higher hydrophobicity, less EPS, and greater attachment efficiency when grown in the manure extract as opposed to LB. The zeta potential was the only physical-chemical parameter tested which was found to be correlated to the attachment efficiency, but only for the isolates grown in LB. This study demonstrated the need to study bacterial pathogens in more representative conditions to accurately portray their behavior in an aquatic environment.

The study described in Chapter 4 was partially motivated by the results observed in Chapters 2 and 3, where a change in the growth conditions elicited an altered phenotypic response in the cells. To further investigate how the environment influences the behavior of pathogens, three *in vitro* systems were built in the lab: a human colon, septic tank, and a groundwater system. These specific environments were recreated in the lab, because they represent a waterborne pathway in which pathogens could infect

people. Initially, the lab-scale human colon and septic tank were tested to ensure that they were able to operate similarly to their complex environment counterparts. The microbial composition and short-chain fatty acid production were tested on the model colon, while microbial composition analysis and water quality tests (total suspended solids, pH, conductivity, hardness, total organic carbon, and biological oxygen demand) were conducted on the model septic tank, which confirmed the efficacy of the simulated systems. The three systems were operated with a fecal microbial community to get a baseline of the microorganisms present (microbial structure), as well as the physical-chemical and transport properties of the cells through porous media (microbial function). An enteric pathogen, *E. coli* O157:H7, was then added to the microbial community in the colon and was subsequently transferred to the septic tank and groundwater systems. The addition of the pathogen in the colon changed the ratio between the two dominant phyla (bacteriodetes and firmicutes), increased the hydrophobicity, and cell size. The aquatic systems also had an increase in cell size, a reduced sugar/protein ratio, and a reduced quantity of proteobacteria. This novel investigation demonstrated the need to study cells under conditions which better simulate real environments where the bacteria of interest are found.

The findings from this dissertation provide the following critical insights into the study of pathogens in the laboratory. First, the growth phase of bacteria may have a major effect on cells' surface characteristics, which may subsequently influence their transport. Second, exposure to different growth solutions will influence the fate and transport of bacteria in often unpredictable ways. Third, pathogenic bacteria should be studied under

conditions as similar to the environments in which the pathogens proliferate to fully capture the organism's response and the resilience of the host community's structure and function.

This dissertation study has demonstrated the need to change the paradigm for studying pathogenic bacteria from ideal to real conditions in order to better understand their fate and transport in the environment. The findings presented in this investigation have the potential to change how researchers study pathogens in the laboratory. Results from these applied techniques may inform new regulations for septic tanks and groundwater system design and management to protect potable water from pathogens. The growing field of metagenomics and single cell analysis techniques would be useful addendums to this work, by studying how the pathogens change genotypically within *in vitro* systems to gain a thorough understanding of bacterial pathogens in the environment.

Appendix A

Supplemental Material for Chapter 2

Zeta Potential Measurements:

The zeta potential of the *Pseudomonas aeruginosa* isolates grown to mid-exponential and stationary phases were measured using a zeta potential analyzer (Brookhaven Instruments Corporation, Holtsville, NY). The cells were first washed and diluted to an optical density of 0.1 (OD_{600}) in 100mM NaCl, as described in the manuscript. The suspended cells are then places in the zeta potential analyzer to be measured. The measurements were repeated ten times for the cells grown to the two growth phases and the average was reported. The Smoluchowski equation was used to calculate the zeta potential from the electrophoretic mobility [1].

Zeta Potential Values:

Pseudomonas aeruginosa	Mid-exponential	Stationary
Zeta Potential (mV)	-16.4 ± 2.1	-11.1 ± 5.5

Growth curve of *Pseudomonas aeruginosa* PAO1 in LB medium:

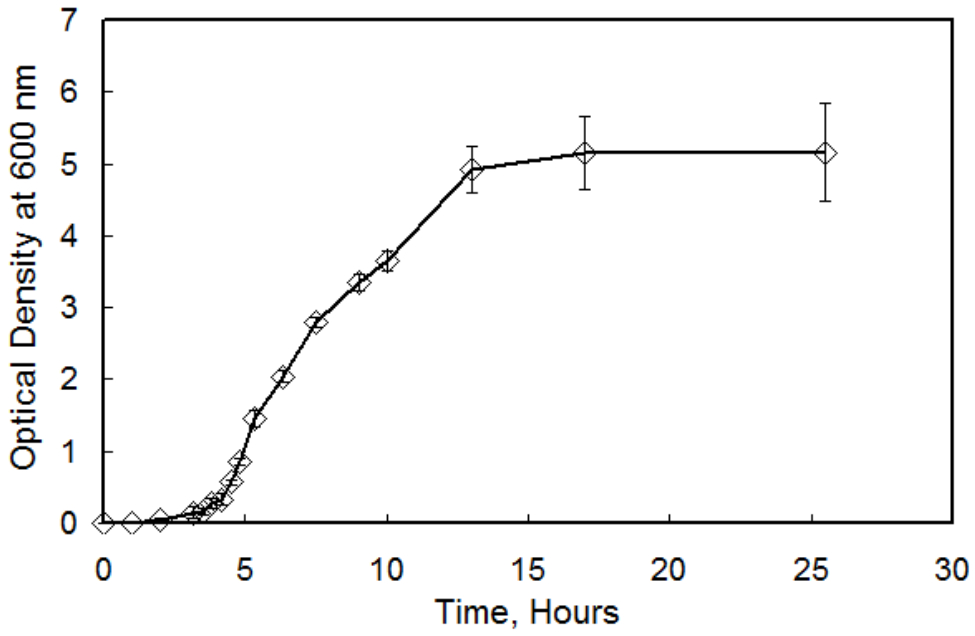

Figure A1.1: Growth curve of P. aeruginosa PAO1 in LB medium at 30 ºC and 150 rpm.

DLVO Theory Applied to Cell-Surface Interaction

Derjaguin–Landau–Verwey–Overbeek (DLVO) theory [2] was applied to evaluate whether the differences in cell attachment to the surface could be attributed to differences in the relative contribution of electrostatic and van der Waal interactions. Interaction profiles for the cell–crystal systems were developed assuming sphere-plate geometry and constant potential model using the following equations [3, 4]:

$$V_{EDL} = \pi\varepsilon_0\varepsilon a_p\left\{2\psi_p\psi_c \ln\left[\frac{1+\exp(-\kappa h)}{1-\exp(-\kappa h)}\right] + (\psi_p^2+\psi_c^2)\ln[1-\exp(-2\kappa h)]\right\} \quad (1)$$

$$V_{vdW} = -\frac{Aa_p}{6h}\left[1+\frac{14h}{\lambda}\right]^{-1} \quad (2)$$

Permittivity of free space (ε_0) and the dielectric constant of water (ε) were assumed to be 8.854×10^{-12} C/V/m and 78.5, respectively [5, 6], a_p is the effective bacterial radius. The effective radius was calculated from a sphere having the equivalent volume as the ellipsoid shaped cells (measured to be 0.56 μm). The Hamaker constant (A_{102}) for the cell–quartz–water system was assumed to be 6.5×10^{-21} J [7]; and κ is the inverse Debye length, which is assumed to be 1.04×10^{9} m^{-1} in an aqueous 100mM NaCl solution [5]. Zeta potential values for the cells used in placed of streaming potentials, ψ_p (-16.4 and -11.1 mV for mid-exponential and stationary cells, respectively) [8] and surfaces, ψ_c (-15.1, and -11.6 for PVDF and SiO_2, respectively) were referenced from the literature [9, 10]. A characteristic dielectric wavelength (λ) of 100 nm was assumed [10]. The following figures were created using DLVO theory with the previously stated parameters.

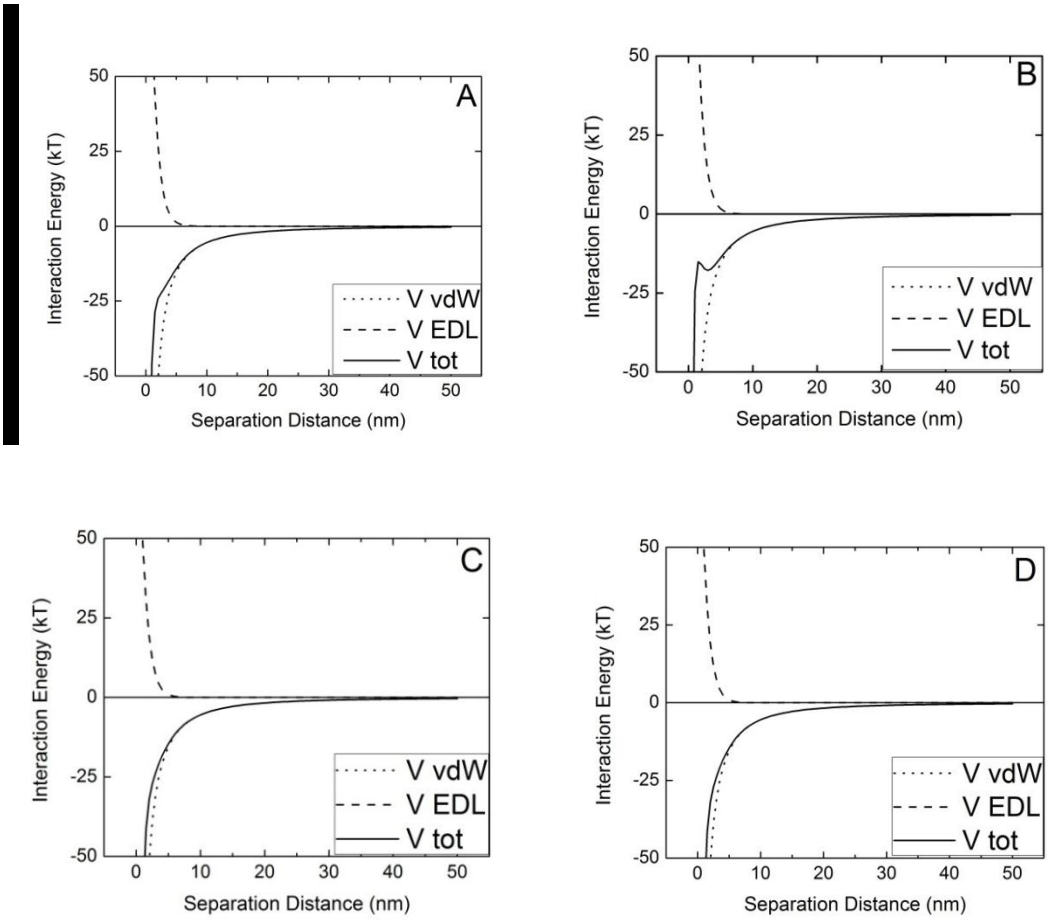

Figure A1.2. These figures displays the DLVO profile of (A) hydrophilic cells (mid-exponential growth phase) interacting with a hydrophilic surface (SiO_2). (B) hydrophilic cells interacting with a hydrophobic surface (PVDF), (C) hydrophobic cells (stationary growth phase) interacting with a hydrophilic surface, and (D) hydrophobic cells interacting with a hydrophobic surface.

It could be inferred from these images that the conditions are favorable no matter the separation distance with no energy barrier, nor secondary minima. All of the cell-surface interactions were favorable according to the DLVO theory. This suggests that there are other cell surface inactions that may explain the varying ways in which the cells attached to the different surfaces in this study.

Representative Fluorescent Microscope Pictures (Stationary Cells on PVDF Surface):

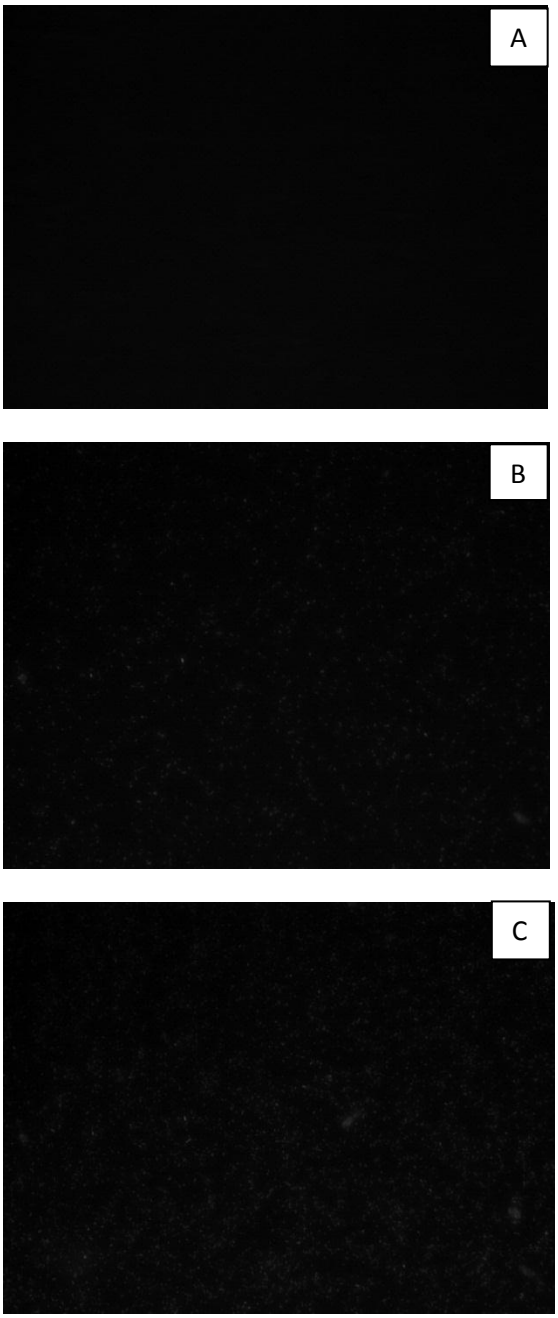

Figure A1.3. These figures display the Stationary cells on PVDF surface after three time intervals, 5, 30, and 60 minutes.

References

1. O'Brien, R. W., and White, L. R. (1978) *Journal of the Chemical Society, Faraday Transactions 2: Molecular and Chemical Physics* **74**
2. Hermansson, M. (1999) *Colloids and Surfaces B: Biointerfaces* **14**, 105-119
3. Hogg, R., Healy, T. W., and Fuerstenau, D. W. (1966) *Transactions of the Faraday Society* **62**, 1638-1651
4. Elimelech, M., and O'Melia, C. R. (1990) *Langmuir* **6**, 1153-1163
5. Elimelech, M., Gregory, J., Jia, X., and Williams, R. A. (1995) Particle Deposition and Aggregation: Measurement, Modeling and Simulation. Butterworth-Heinemann. pp 441
6. Hong, Y., Honda, R. J., Myung, N. V., and Walker, S. L. (2009) *Environmental Science & Technology* **43**, 8834-8839
7. Simoni, S. F., Bosma, T. N. P., Harms, H., and Zehnder, A. J. B. (2000) *Environmental Science & Technology* **34**, 1011-1017
8. Bruinsma, G. M., Rustema-Abbing, M., van der Mei, H. C., and Busscher, H. J. (2001) *Journal of Microbiological Methods* **45**, 95-101
9. Pasmore, M., Todd, P., Smith, S., Baker, D., Silverstein, J., Coons, D., and Bowman, C. N. (2001) *Journal of Membrane Science* **194**, 15-32
10. Redman, J. A., Walker, S. L., and Elimelech, M. (2004) *Environmental Science & Technology* **38**, 1777-1785

Appendix B

Representations of Experimental Set-ups

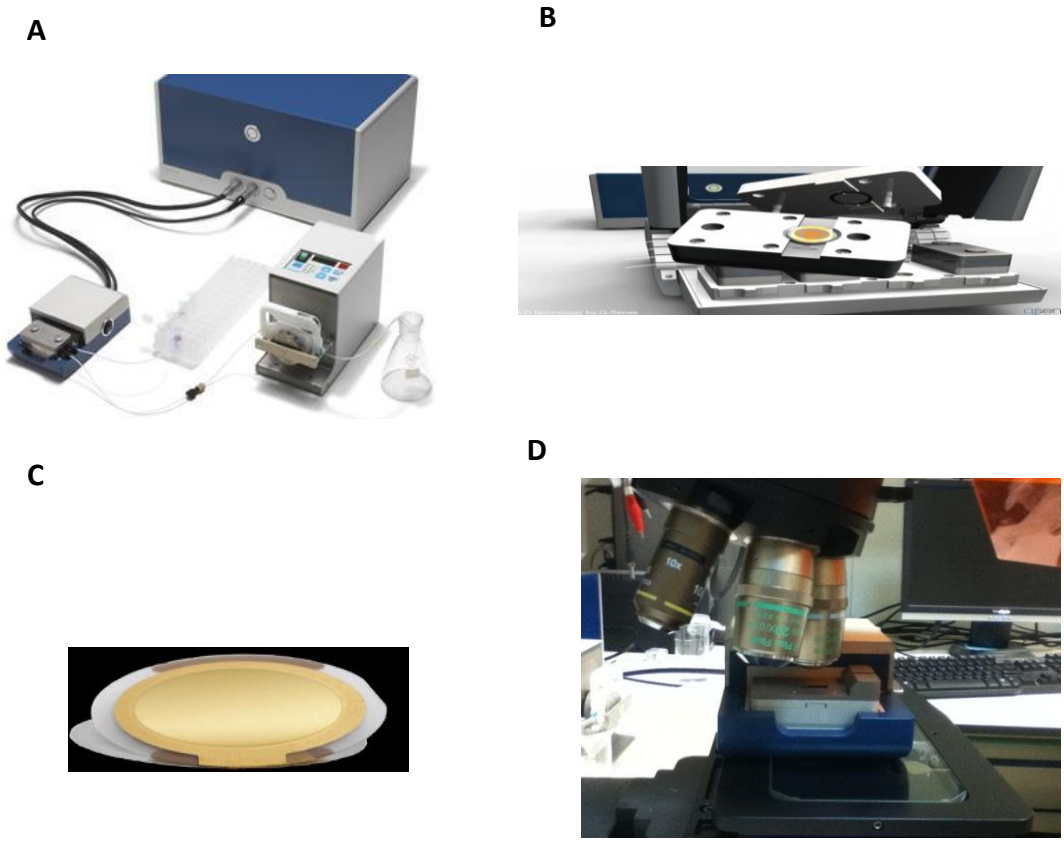

Figure B1. Pictures of the a quartz crystal microbalance with dissipation setup used in Chapter 2. QCM-D (A), operating chamber (B), quartz crystal surface (C), and the full setup with a fluorescent microscope (D).

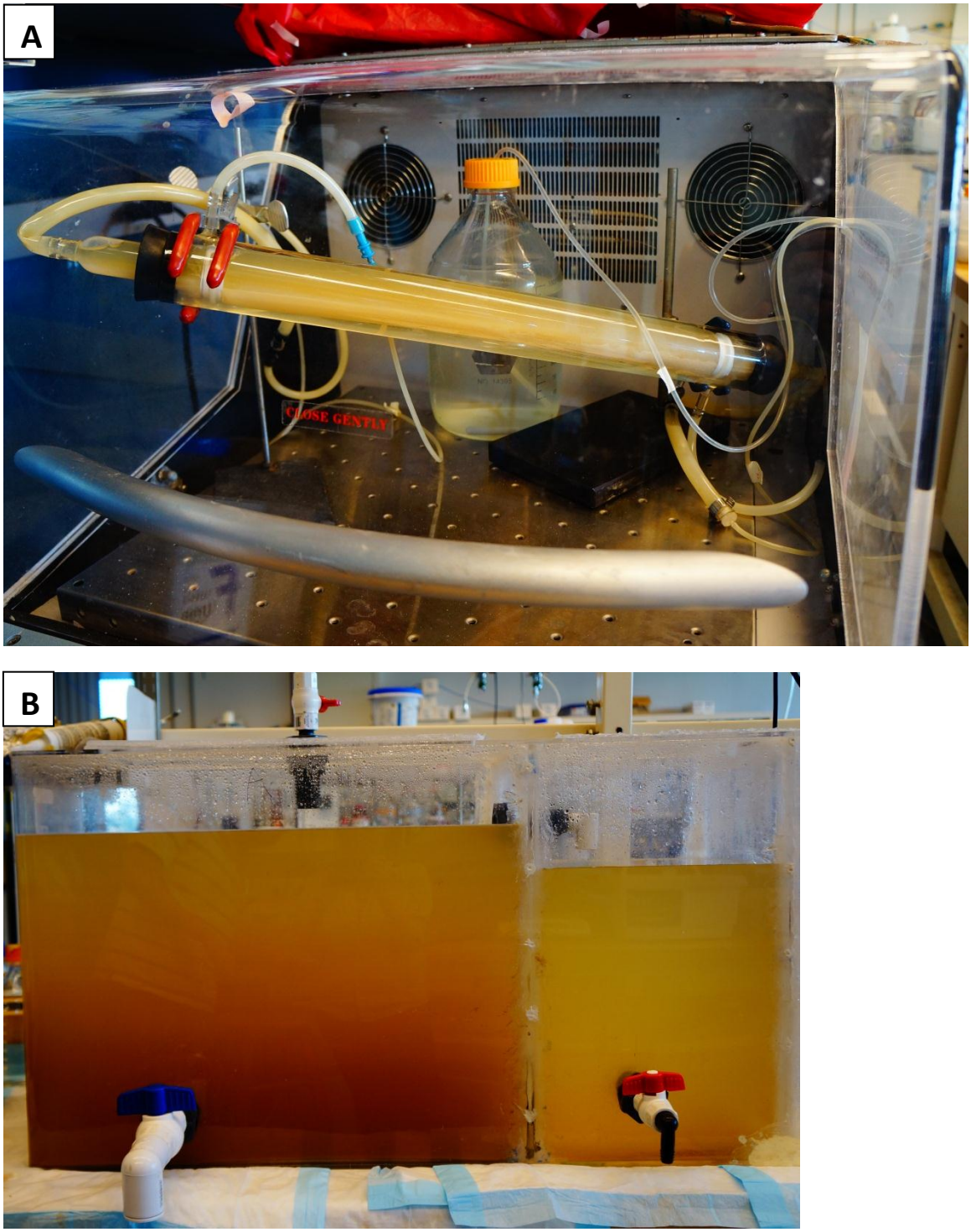

Figure B2. Picture of the model colon (A) and model septic tanks (B) used in Chapter 4.